NONLINEAR MECHANICAL SYSTEM WITH AN IMPACT VIBRATION ABSORBER

STEADY STATE RESPONSE OF A NON-LINEAR MECHANICAL SYSTEM PROVIDED WITH AN IMPACT VIBRATION ABSORBER

By

SUNIL KUMAR JHA, B.Sc. (Eng.), D.R.C.

A Thesis

Submitted to the Faculty of Graduate Studies

in Partial Fulfilment of the Requirements

for the Degree

Master of Engineering

McMaster University

September 1966

MASTER OF ENGINEERING (1966)
(Mechanical Engineering)

McMASTER UNIVERSITY
Hamilton, Ontario.

TITLE: Steady State Response of a Non-linear Mechanical System Provided with an Impact Vibration Absorber

AUTHOR: Sunil Kumar Jha, B.Sc. (Eng.) (University of Glasgow)
D.R.C. (University of Strathclyde)

SUPERVISOR: Dr. M. A. Dokainish

NUMBER OF PAGES: viii, 111

SCOPE AND CONTENTS:

An investigation of the steady state response of a non-linear system (having bi-linear restoring force characteristic) provided with an impact vibration absorber is made.

The effect of two main parameters viz. clearance d_o and mass ratio $\mu = \frac{m}{M}$ on amplitude of vibration of the system has been investigated experimentally over a range of frequency.

A numerical analysis of the problem has been made with a digital computer to supplement the experimental results.

ABSTRACT

An investigation of the steady state response of a non-linear system provided with an impact vibration absorber is made. The term non-linear in the present case refers to a system in which the spring restoring force is bi-linear.

The effect of two main parameters viz. clearance d_o (i.e. the free path of travel of the mass particle) and mass ratio $\mu = \frac{m}{M}$ (i.e. mass ratio between the mass particle and the primary system) on amplitude of vibration of the system has been investigated experimentally over a range of frequency.

A numerical analysis of the problem is made with the aid of a digital computer to supplement the experimental results.

It has been found that with proper choice of parameters an impact vibration absorber is effective in reducing vibration level of a non-linear system undergoing sinusoidal excitation.

ACKNOWLEDGEMENTS

The author wishes to express his thanks to the Department of Mechanical Engineering for the permission to make use of the research facilities provided in the Dynamics Laboratory of the University.

The author is deeply grateful to his supervisor Dr. M. A. Dokainish, for his constant assistance, guidance and encouragement during this investigation.

The author also expresses his gratitutde to Dr. D. J. Kenworthy for his help and suggestions relating computation work.

Thanks are due to staff of the Mechanical Engineering Laboratories for their assistance in building the test rig and to Miss Ada van der Dussen for her expert typing.

The author is further indebted to the Department of Mechanical Engineering for the award of the scholarship and assistantship.

This study was supported by National Research Council Grant No. A-2726, and the author gratefully acknowledges the receipt of the same.

NOMENCLATURE

A = maximum displacement amplitude of primary system in the absence of the impact vibration absorber (in.)

c = damping coefficient (lb.sec/in)

d = damping factor, $c/2M\ p_1$

d_o = clearance in which the mass particle is free to oscillate (in.)

e = coefficient of restitution

F = maximum force of excitation (lb.)

K_1 = equivalent stiffness of the leaf springs in the region where their motion is not constrained by the guide block (lb./in.)

K_2 = equivalent stiffness of the leaf springs in the region where their motion is constrained by the guide blocks (lb./in.)

M = mass of primary system (lb.sec.^{2}/in.)

m = mass of particle (lb.sec.^{2}/in.)

p_1 = $\sqrt{K_1/M}$

t = time (sec.)

v = absolute velocity of particle (in./sec.)

x = displacement of M (in.)

x_a = displacement of M immediately after impact (in.)

x_b = displacement of M immediately before impact (in.)

y_1 = displacement of particle (in.)

y = relative displacement of particle with respect to M (in.)

ψ = phase angle due to damping (rad)

μ = mass ratio, m/M

ω = forcing frequency (rad/sec.)

$\cdot = \frac{d}{dt}$

$\cdot\cdot = \frac{d^2}{dt^2}$

N.B. The units in the parentheses are the units which have been normally used unless otherwise stated.

1. INTRODUCTION

1.1 Historical Review of Impact Vibration Absorber

An impact vibration absorber consists of a mass particle within a container and is free to move relative to the container. During oscillation the mass particle withdraws energy from the system and dissipates it through impact.

The idea of reducing vibration by impact was first conceived and investigated by Lieber and Jensen[(1)*] in 1944. In that investigation the authors assumed that the steady state motion of an undamped single degree of freedom system with an impact vibration absorber (referred to as an "acceleration damper") was still simple harmonic, the elastic rebound between the mass particle and its container was zero, and two impacts take place at opposite sides of the container during the time period of the sinusoidal excitation. From the consideration of total work done per cycle on the system they develop a theory and show that for most efficient operation of the vibration absorber (i.e. for maximum energy dissipation) the clearance (i.e. free path of travel) of the mass particle should be π times the maximum amplitude of response of the system.

Grubin[(2)], under assumption of the existance of symmetric 2 impacts per cycle motion determined the behaviour of a viscously damped system after many impacts.

---

* Numbers in parentheses designate references at the end of the thesis.

Arnold[3], also assumed the existance of symmetric 2 impacts per cycle motion and developed a theory for an undamped system representing the impact force by Fourier series. His theoretical investigation was supplemented by experimental studies.

Warbarton[4], gave a method to obtain a solution for 2 impacts per cycle motion, in which consideration of only two successive impacts are needed.

Kaper[5], investigated the problem in order to determine the effectiveness of impact vibration absorber (referred to as "discontinuous dynamic vibration absorber") in the case of free vibrations as well as forced vibrations due to sinusoidal excitation.

Masri[6], in his investigation obtained a solution for symmetric 2 impacts per cycle motion and determined the stability boundaries for the same.

A number of experimental studies has also been made to this effect to establish the practical feasibility of particle damping. To mention the name of the investigators at this end are McGoldrick[7], who investigated its effect on ship hulls; Lieber and Tripp[8], investigated its effect on cantilever beam, Sankey[9], studied its effect on single degree of freedom systems and Duckwald[10], studied its effect in reducing the vibration of turbine buckets.

1.2 Objective

The objective of the present study is to investigate the behaviour (response characteristic) of a system (having bi-linear restoring force characteristic) provided with an impact vibration absorber, when the system is subjected to a sinusoidal excitation, and to study the effects of parameter variation (viz. clearance d_o and mass ratio μ) on the amplitude of vibration.

The experimental studies that were conducted with a mechanical model are described and their results interpreted in Chapter 2. The theoretical results obtained numerically and their comparison with the experimental ones are to be found in Chapter 3. Discussion of the results and conclusions drawn therefrom are given in Chapter 4.

The derivation of the equation of motion of the system and its steady state solution between impacts is included in Appendix I. Using this result the resulting motion of the system after any impact has been obtained by numerical method. A detailed procedure of this, following the method suggested in reference (6), is outlined in Appendix II.

2. EXPERIMENTAL STUDIES

2.1 Introduction

This study was carried out in order to obtain

a) a physical insight of the phenomena that occurs when a non-linear system provided with an impact vibration absorber is subjected to a sinusoidal excitation,

b) to evaluate the efficiency of the system as a vibration absorbing device,

c) to study the effect of parameter variation (viz. d_o and μ) on the amplitude response of the system,

d) to get an idea of the design problems that may be encountered in the actual construction of such a device.

2.2 Mechanical Model

Figure 1 shows a mathematical model of the system. It is well-known that the qualitative response of a single degree of freedom oscillating system is not altered if the excitation is applied to the foundation (i.e. at which the oscillating system is resting). instead of directly to the mass. Therefore, for the sake of convenience the former type of excitation was adopted. A schematic diagram of this mechanical model is shown in Figure 2. The photograph of test rig and actual model is shown in Figures 3 and 4 respectively.

Here the main mass M was a rectangular box-like thing, comprising

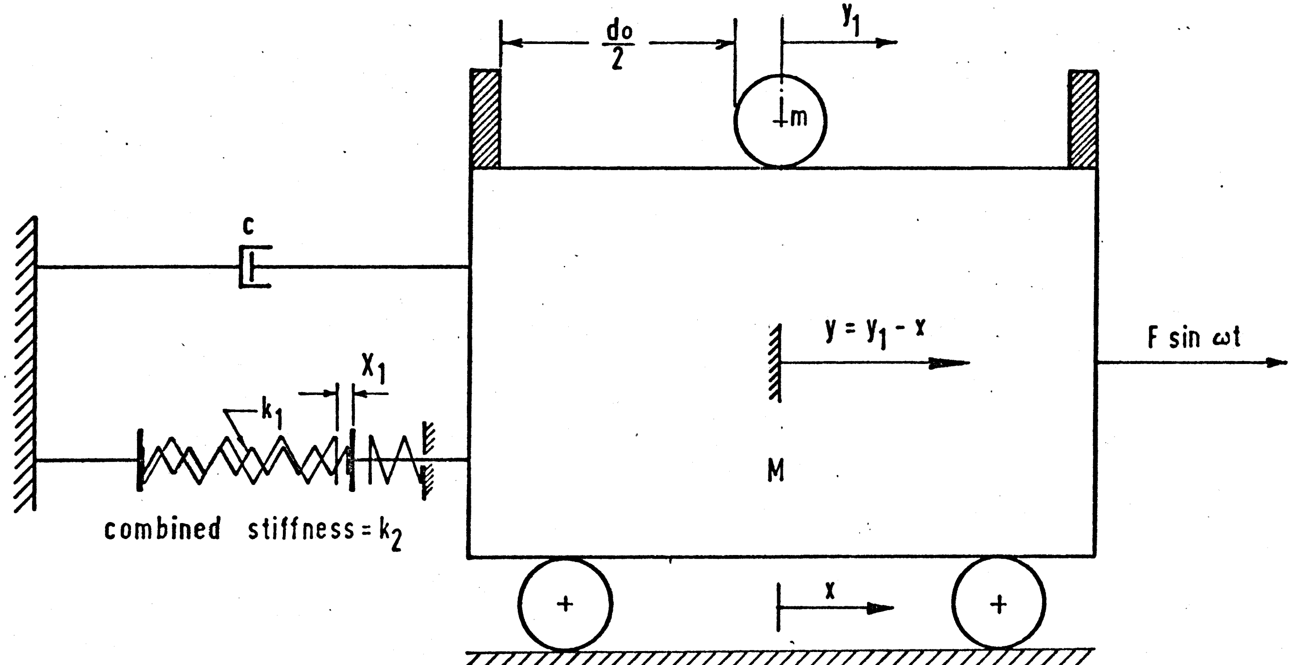

MODEL OF THE SYSTEM

Fig. 1

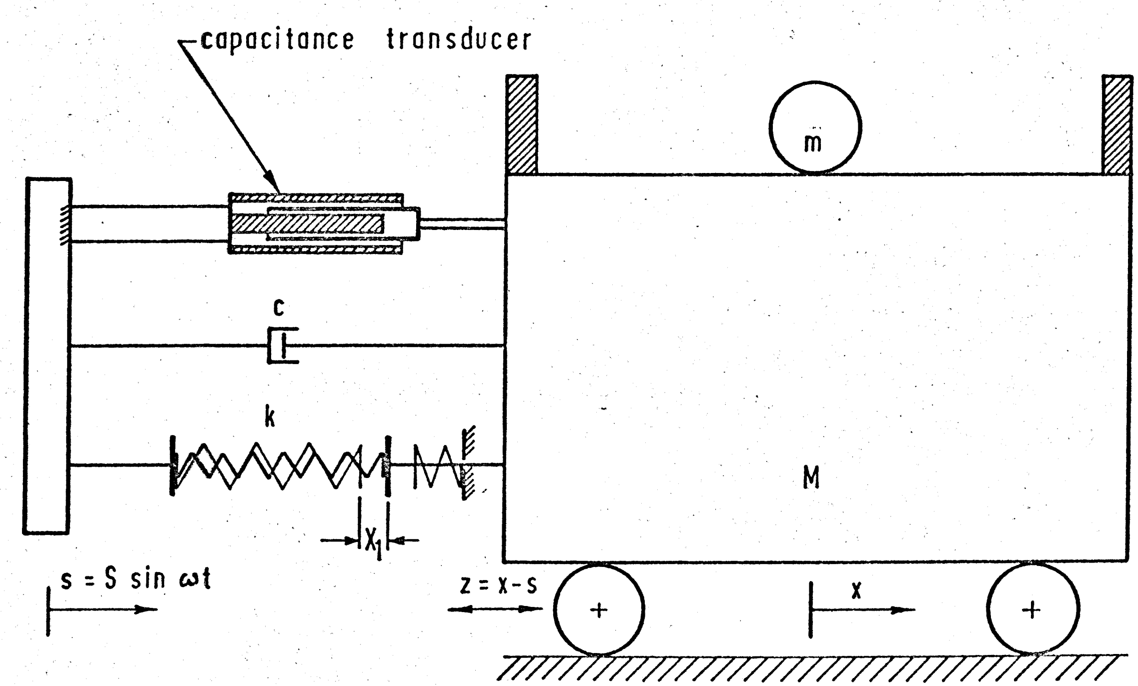

MECHANICAL MODEL

Fig. 2

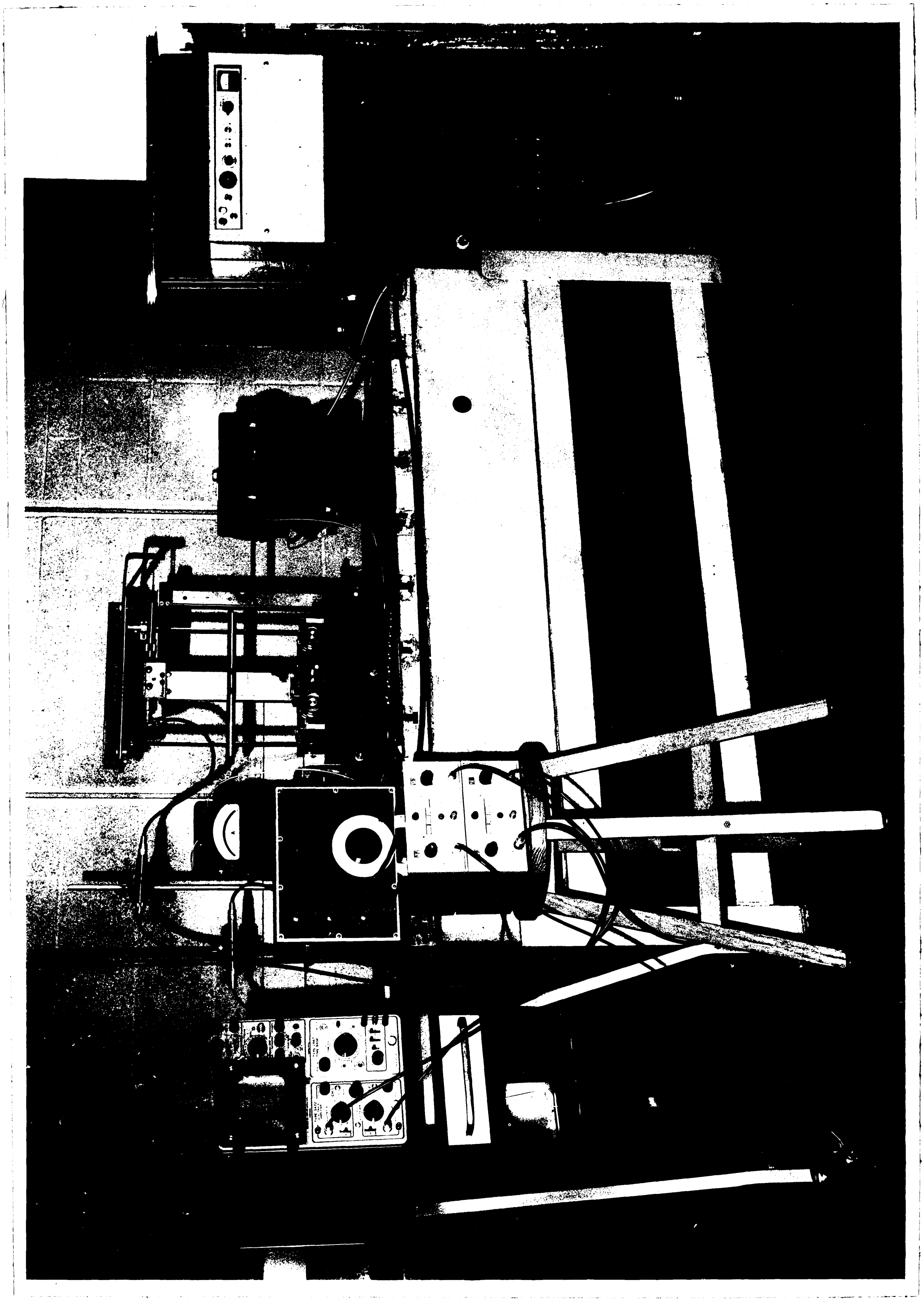

Fig. 3 - General View of the Test Rig

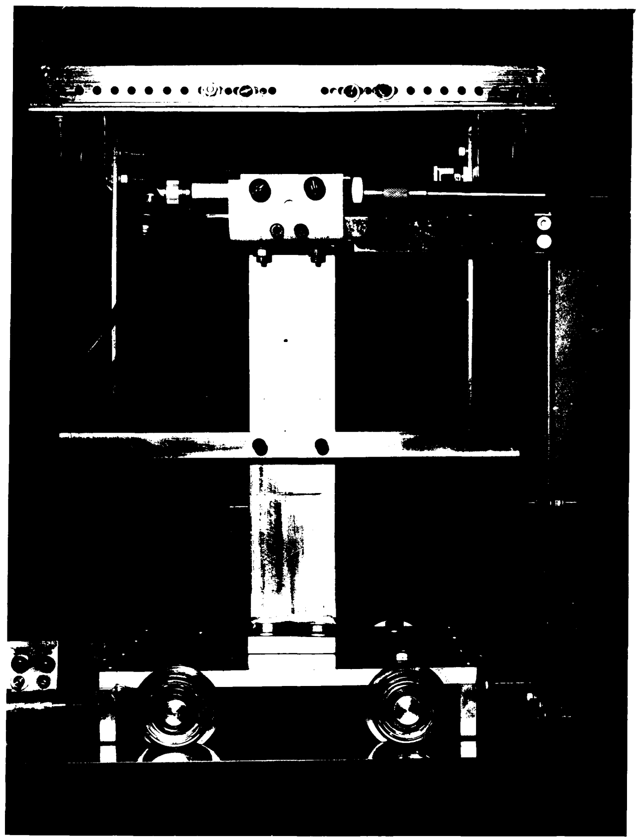

Front View

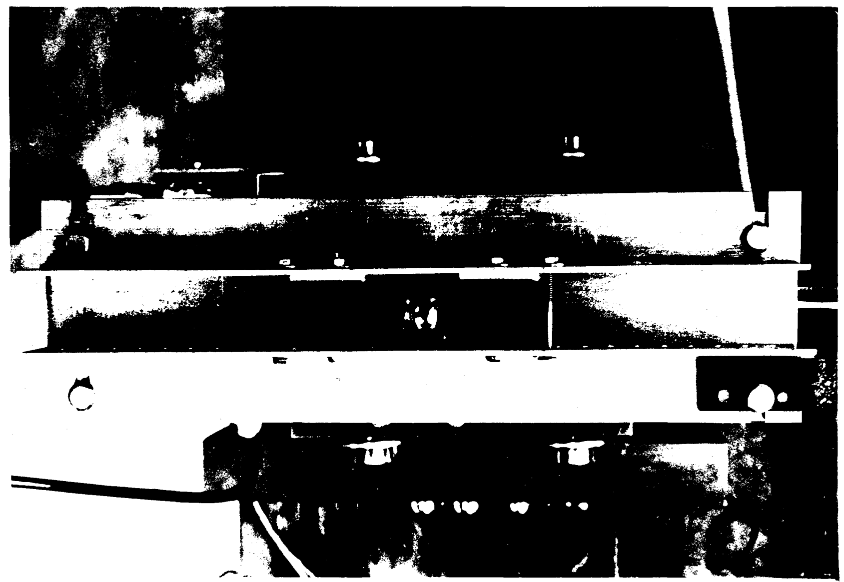

Top View

Fig.4 - Mechanical Model

a base plate, two L-channels and two rigid stops, inside which the frictionless mass particle can oscillate. The mass particle used in this case was a hardened steel ball that is usually used in ball-bearings. The stops upon which ball made collission were of mild steel but had been case hardened so as to obtain high coefficient of restitution.

The introduction of non-linearity (bi-linear in this case) in the spring stiffness of the system was achieved by using a sliding guide block having two symmetrical rectangular holes. Inside each of these holes was another rectangular block having a slit of necessary dimensions. There were ample clearances between the inside dimensions of the rectangular holes in the main block and the outside dimensions of the smaller blocks so that the smaller blocks can be fixed in a proper position by means of screws in order to obtain exactly the same stiffness for both positive and negative direction motion of the primary system. The main block can slide (concentrically) in a vertical axis over a rectangular beam, which is rigidly fixed to the foundation and can be fixed at any desired height, thus giving flexibility in choice of spring stiffness.

The foundation (which rested on two spindle comprising four wheels, ball-bearings in this case and was made to roll over two rails) was set to excitation by an electromagnetic shaker, and the relative motion between the foundation and the mass M was monitored by means of a capacitance transducer, the output of which was displayed on a cathode-ray-oscilloscope, and measurements were made from its trace height.

Among the difficulties which were encountered as far as proper operation of the mechanical system is concerned, the major one was, above a certain value of excitation force the system started giving rocking motion (a motion about a lateral axis) within a certain frequency range. This was overcome by shifting the point of application of excitation to a higher position than that it originally was.

The experiments were performed with no ball (this gives the response characteristic of the system without a vibration absorber) and with ball sizes of diameter 5/8", 3/4", 7/8", 1", 1 1/8", 1 1/4", 1 3/8" and 1 1/2" and with various clearances. The result of no ball experiment is shown in Figure 5 together with its theoretical equivalent.

In order to gain some knowledge of the effect of parameter variation (d_o and μ) on the response characteristic of the system, experimental work was divided into two parts:

a) experiments, keeping ball size constant and varying clearances (this gives a measure of the effectiveness of gap factor $\frac{d_o}{A}$).

b) experiments, keeping clearance the same and varying ball sizes (this gives a measure of effectiveness of mass ratio μ).

2.3 Experiments with Same Ball but Different Clearances

These experiments were performed with balls of diameter 5/8", 3/4", 7/8", 1", 1 1/4" and 1 1/2" and for seven to ten different clearances in each case. A sample of such results with 1" diameter ball for 4 different clearances is given in tabular form in Appendix III. A summary of experimental results (i.e. the maximum amplitude obtained with a ball for a certain clearance within the frequency range under

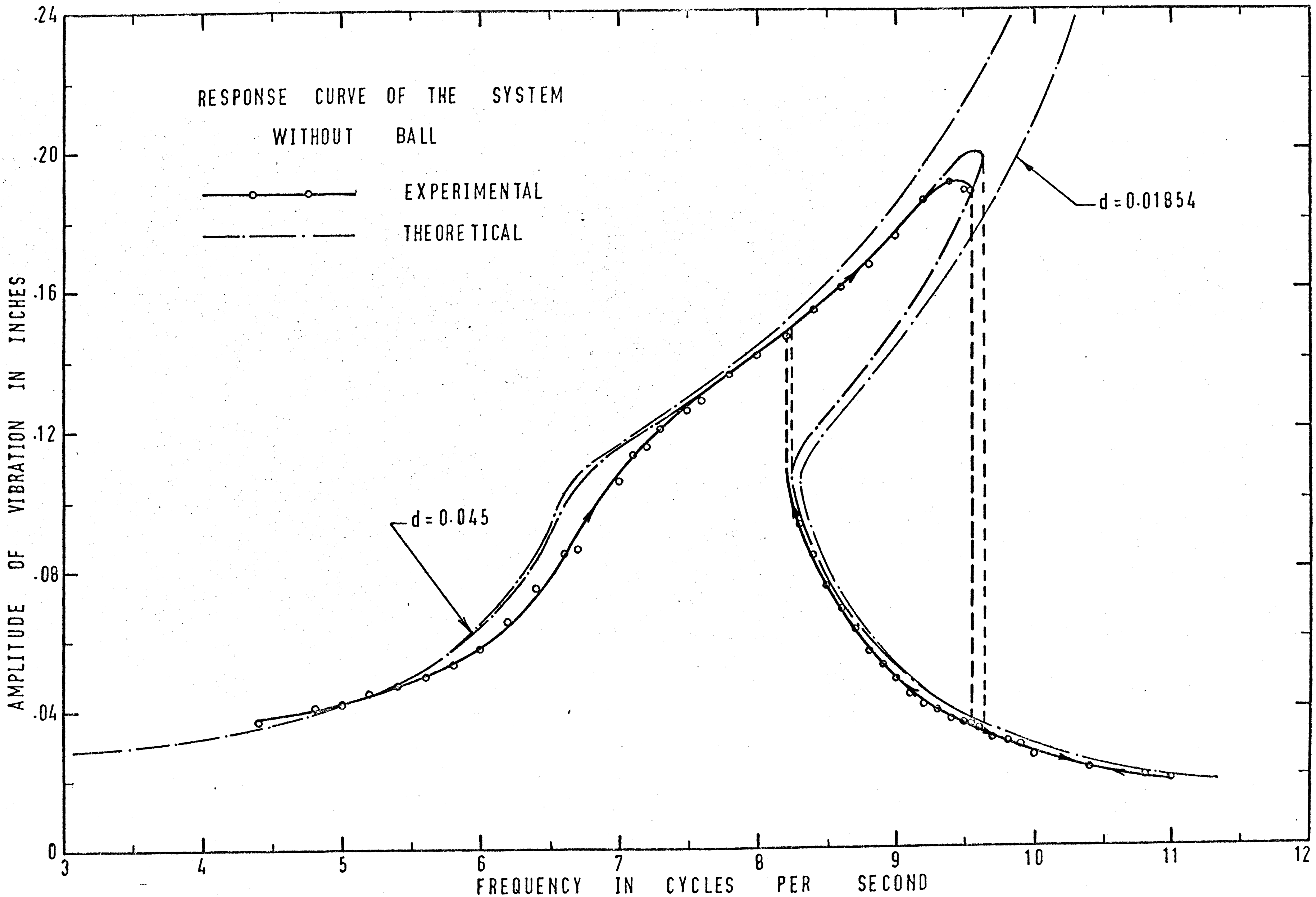

RESPONSE CURVE OF THE SYSTEM
WITHOUT BALL
EXPERIMENTAL
THEORETICAL
d = 0.01854
d = 0.045
AMPLITUDE OF VIBRATION IN INCHES
FREQUENCY IN CYCLES PER SECOND
.24
.20
.16
.12
.08
.04
0
3
4
5
6
7
8
9
10
11
12

Fig. 5

consideration) for each of these tests is given in Appendix IV.A.

In Figures 6 - 11 a few of the test results with different balls and 2 - 3 different clearances have been plotted and these show amplitude response of the system. From these plotted results it is seen that the clearance (or gap factor) has an appreciable effect on amplitude response of the system.

Figure 12 in which amplitude ratio $(\frac{X}{A})_{max}$ has been plotted against $(\frac{d_o}{A})$ for different balls summarises the experimental results thus obtained and gives a more clear and convincing picture of effectiveness of gap factor on amplitude of vibration. Figure 12.1 shows a curve of optimum design parameters, the data for which was obtained from Figure 12.

2.4 Experiments with Same Clearance but Different Balls

These experiments were performed for three different clearances (d_o = 0.351, 0.403, 0.500 inch) with six to seven different balls. The response curves for each of these with two different ball sizes are shown in Figures 13 - 15. A summary of experimental results (i.e. maximum amplitude for a particular configuration within the frequency range under consideration) obtained from each of these tests are tabulated in Appendix IV.B. These results are plotted in Figure 16 as amplitude ratio $(\frac{X}{A})_{max}$ against mass ratio μ and show (for a particular clearance) the effectiveness of mass ratio on the amplitude response of the system.

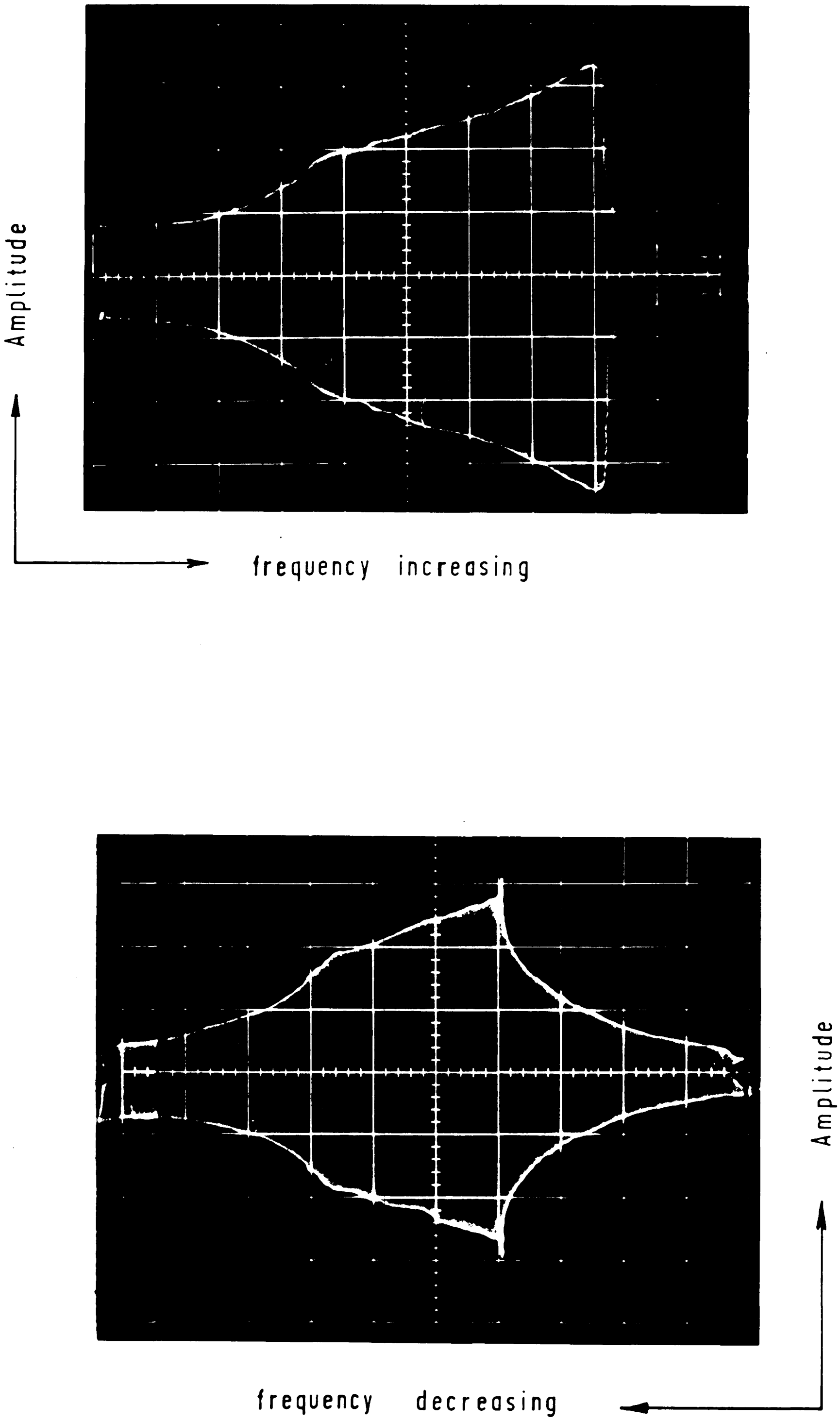

Fig. 5.1 - Jump Phenomena [Qualitative Response]

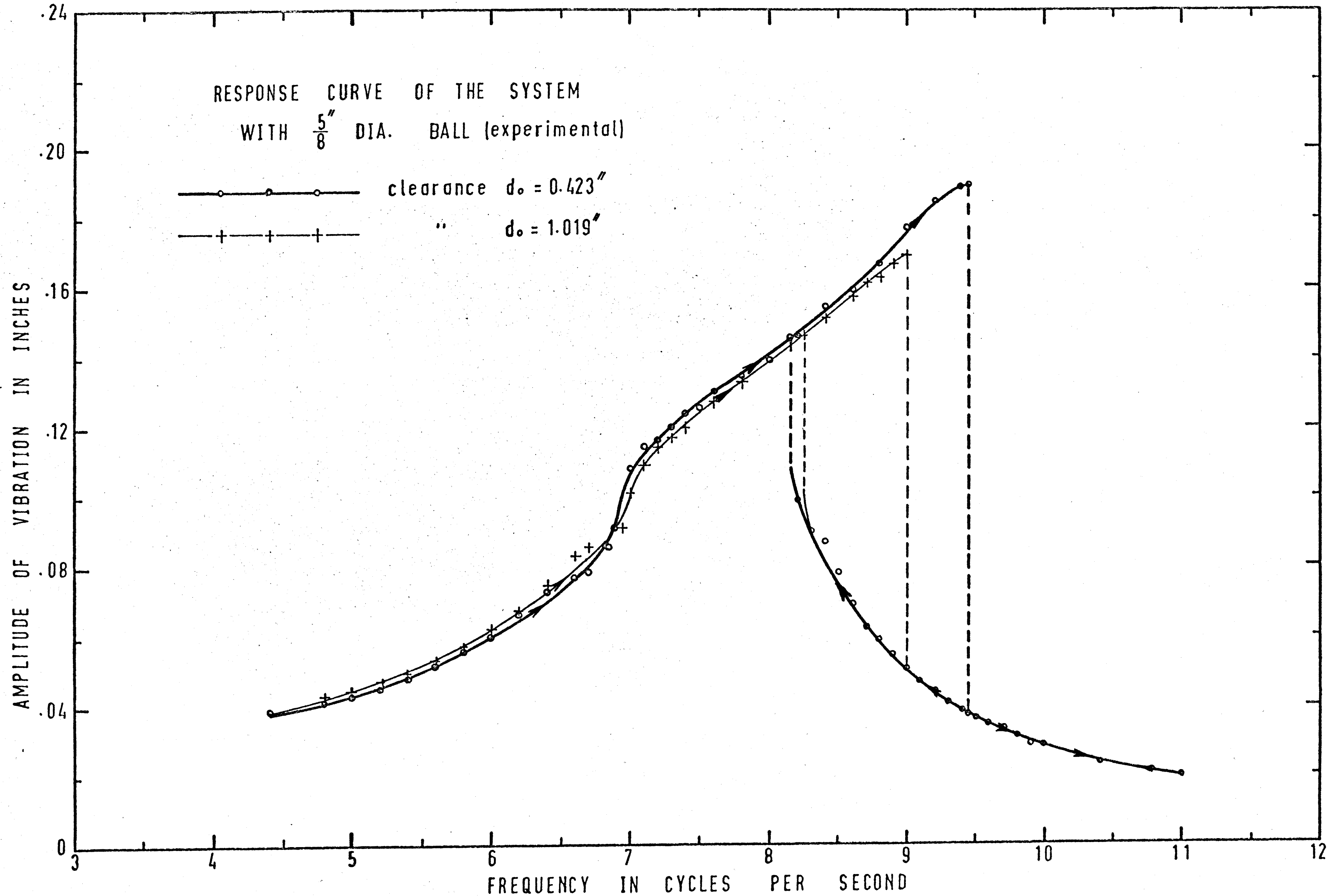
RESPONSE CURVE OF THE SYSTEM
WITH 5/8" DIA. BALL (experimental)
clearance d₀ = 0.423"
" d₀ = 1.019"
AMPLITUDE OF VIBRATION IN INCHES
FREQUENCY IN CYCLES PER SECOND
.24
.20
.16
.12
.08
.04
0
3
4
5
6
7
8
9
10
11
12

Fig. 6

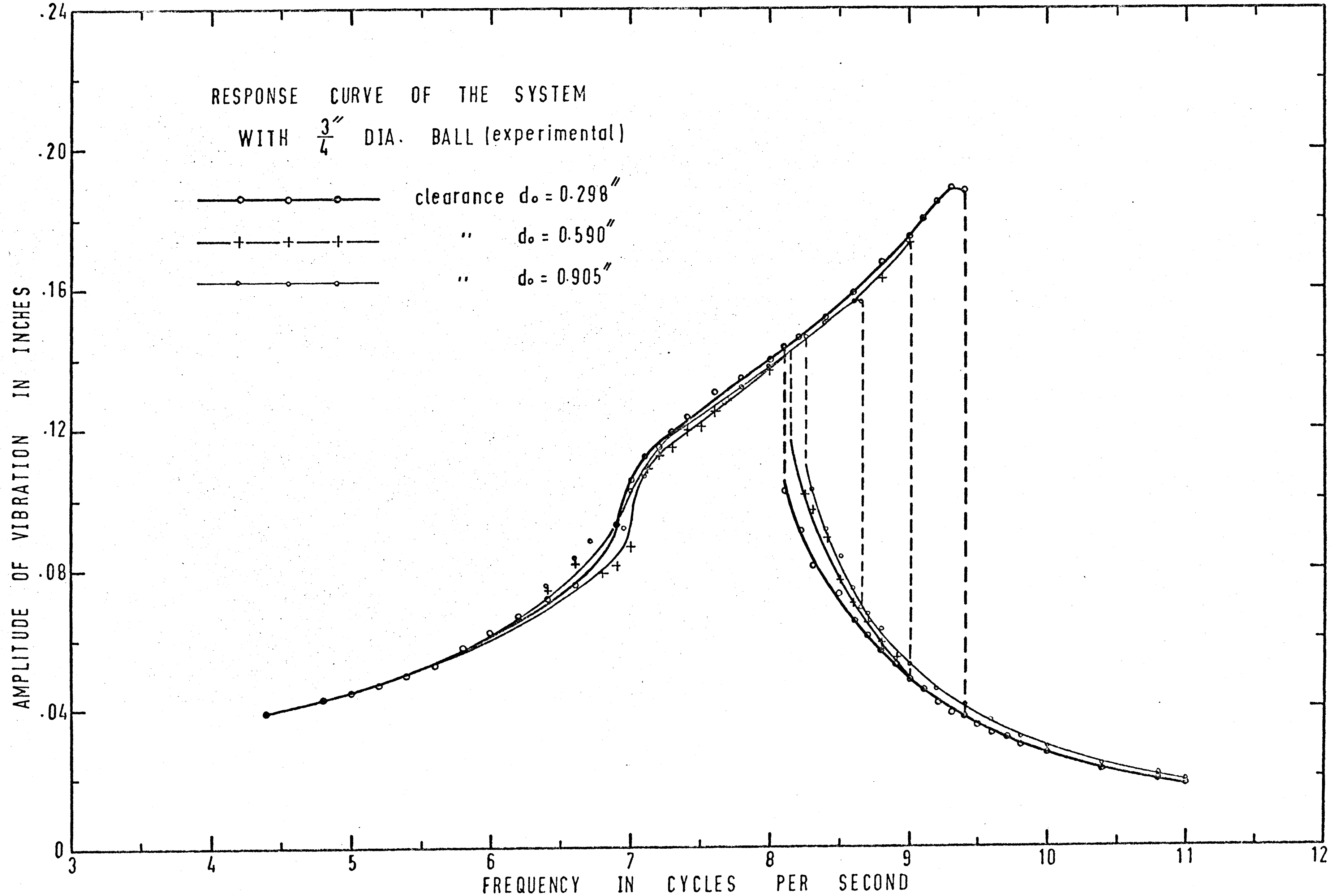
RESPONSE CURVE OF THE SYSTEM
WITH 3/4" DIA. BALL (experimental)
clearance do = 0.298"
" do = 0.590"
" do = 0.905"
AMPLITUDE OF VIBRATION IN INCHES
.24
.20
.16
.12
.08
.04
0
3
4
5
6
7
8
9
10
11
12
FREQUENCY IN CYCLES PER SECOND

Fig. 7

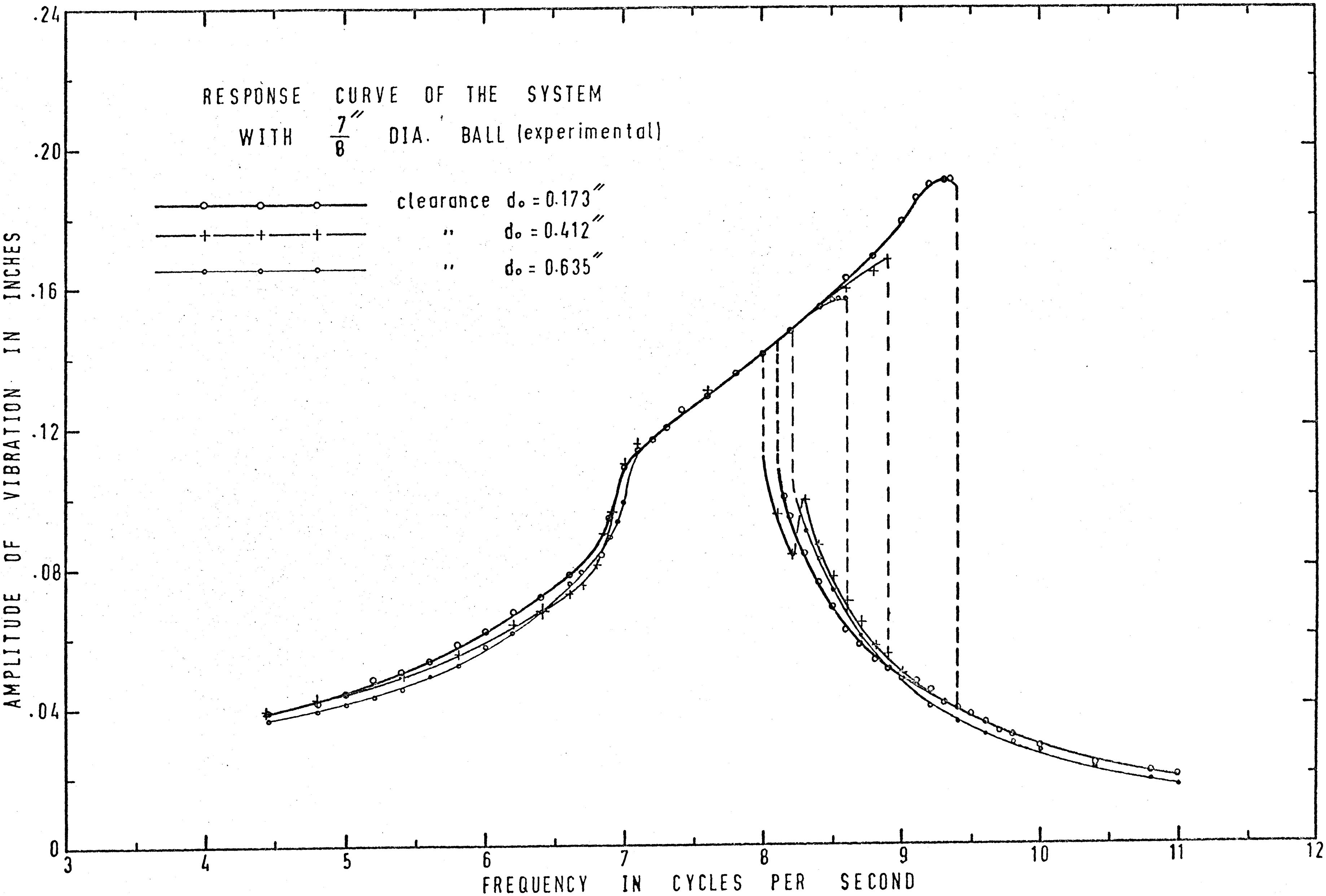
RESPONSE CURVE OF THE SYSTEM
WITH 7/8" DIA. BALL (experimental)
clearance d₀ = 0.173"
" d₀ = 0.412"
" d₀ = 0.635"
AMPLITUDE OF VIBRATION IN INCHES
FREQUENCY IN CYCLES PER SECOND
.24
.20
.16
.12
.08
.04
0
3
4
5
6
7
8
9
10
11
12

Fig. 8

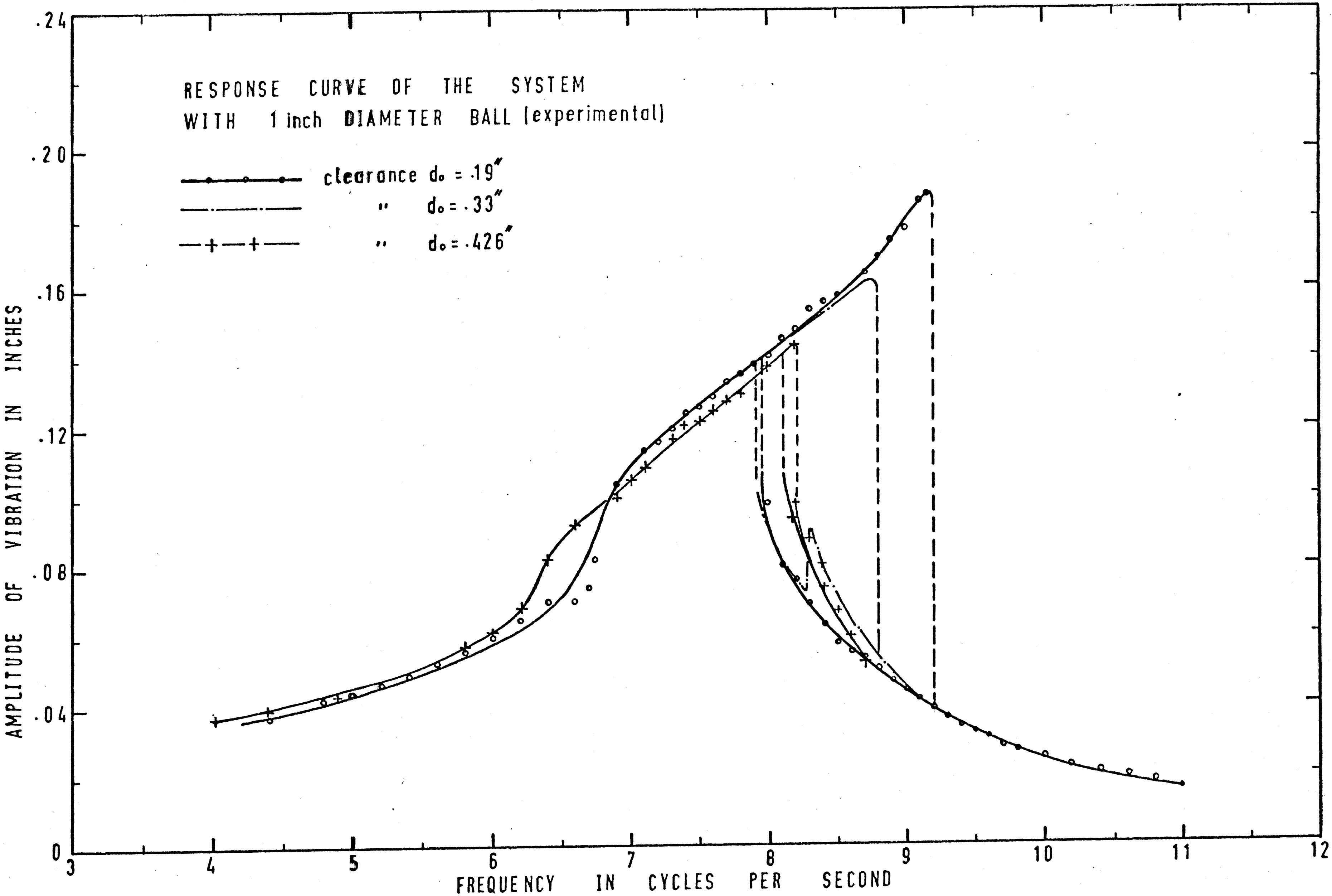
RESPONSE CURVE OF THE SYSTEM
WITH 1 inch DIAMETER BALL (experimental)
clearance d₀ = .19"
" d₀ = .33"
" d₀ = .426"
AMPLITUDE OF VIBRATION IN INCHES
FREQUENCY IN CYCLES PER SECOND
.24
.20
.16
.12
.08
.04
0
3
4
5
6
7
8
9
10
11
12

Fig. 9

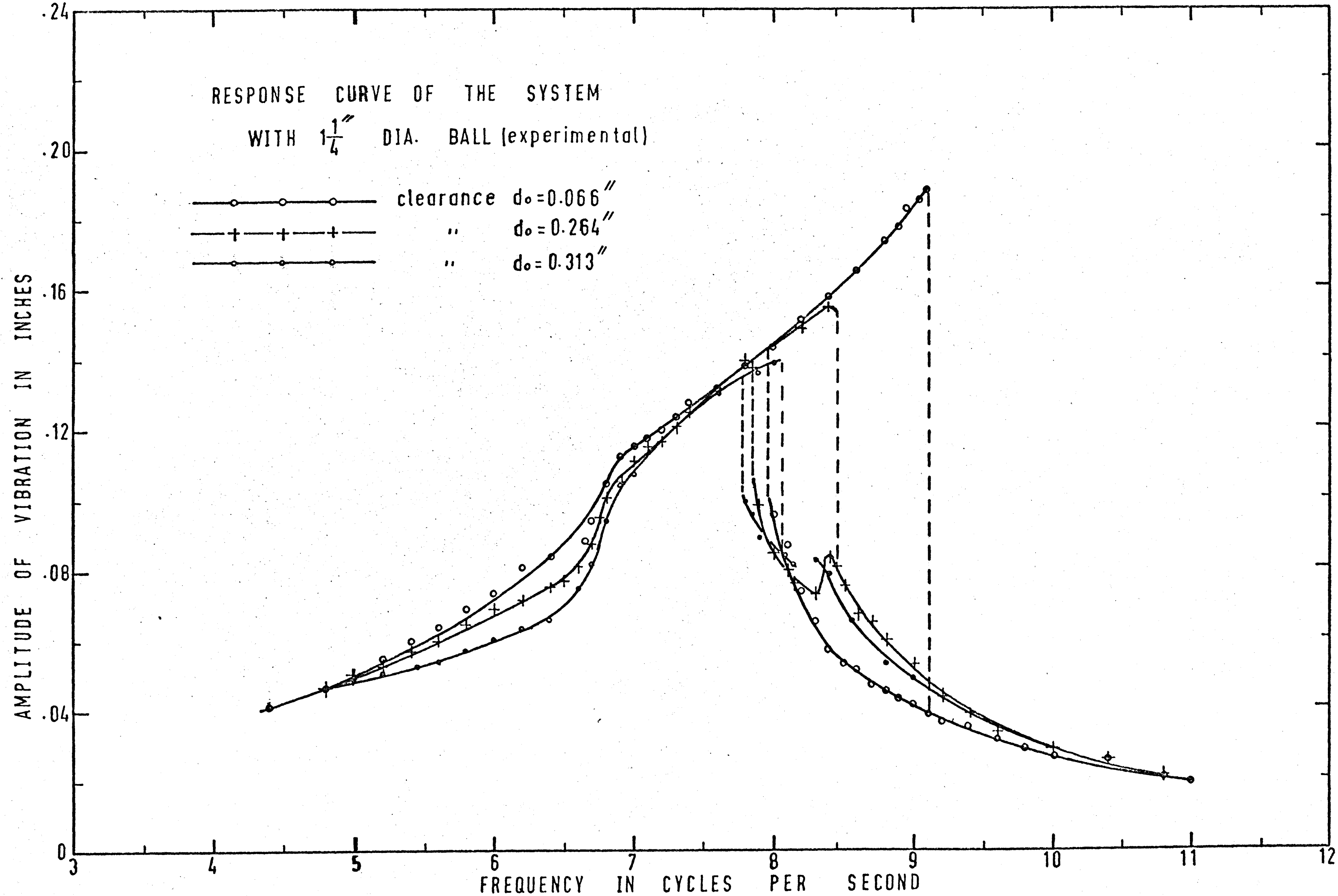
RESPONSE CURVE OF THE SYSTEM
WITH 1 1/4″ DIA. BALL (experimental)
clearance d₀=0.066″
″ d₀=0.264″
″ d₀=0.313″
AMPLITUDE OF VIBRATION IN INCHES
FREQUENCY IN CYCLES PER SECOND
.24
.20
.16
.12
.08
.04
0
3
4
5
6
7
8
9
10
11
12

Fig. 10

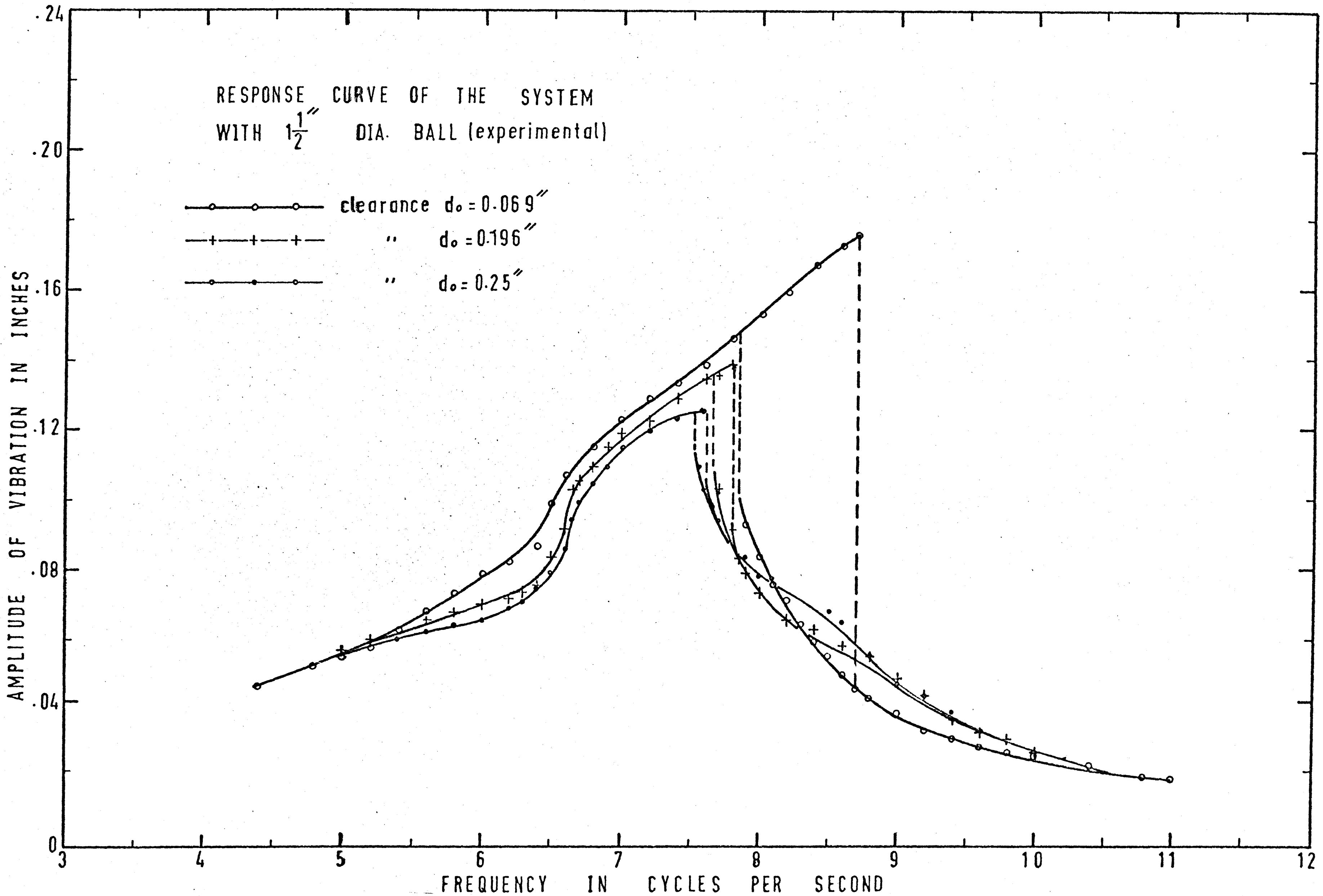
RESPONSE CURVE OF THE SYSTEM
WITH $1\frac{1}{2}''$ DIA. BALL (experimental)
clearance $d_o = 0.069''$
" $d_o = 0.196''$
" $d_o = 0.25''$
AMPLITUDE OF VIBRATION IN INCHES
.24
.20
.16
.12
.08
.04
0
3
4
5
6
7
8
9
10
11
12
FREQUENCY IN CYCLES PER SECOND

Fig.11

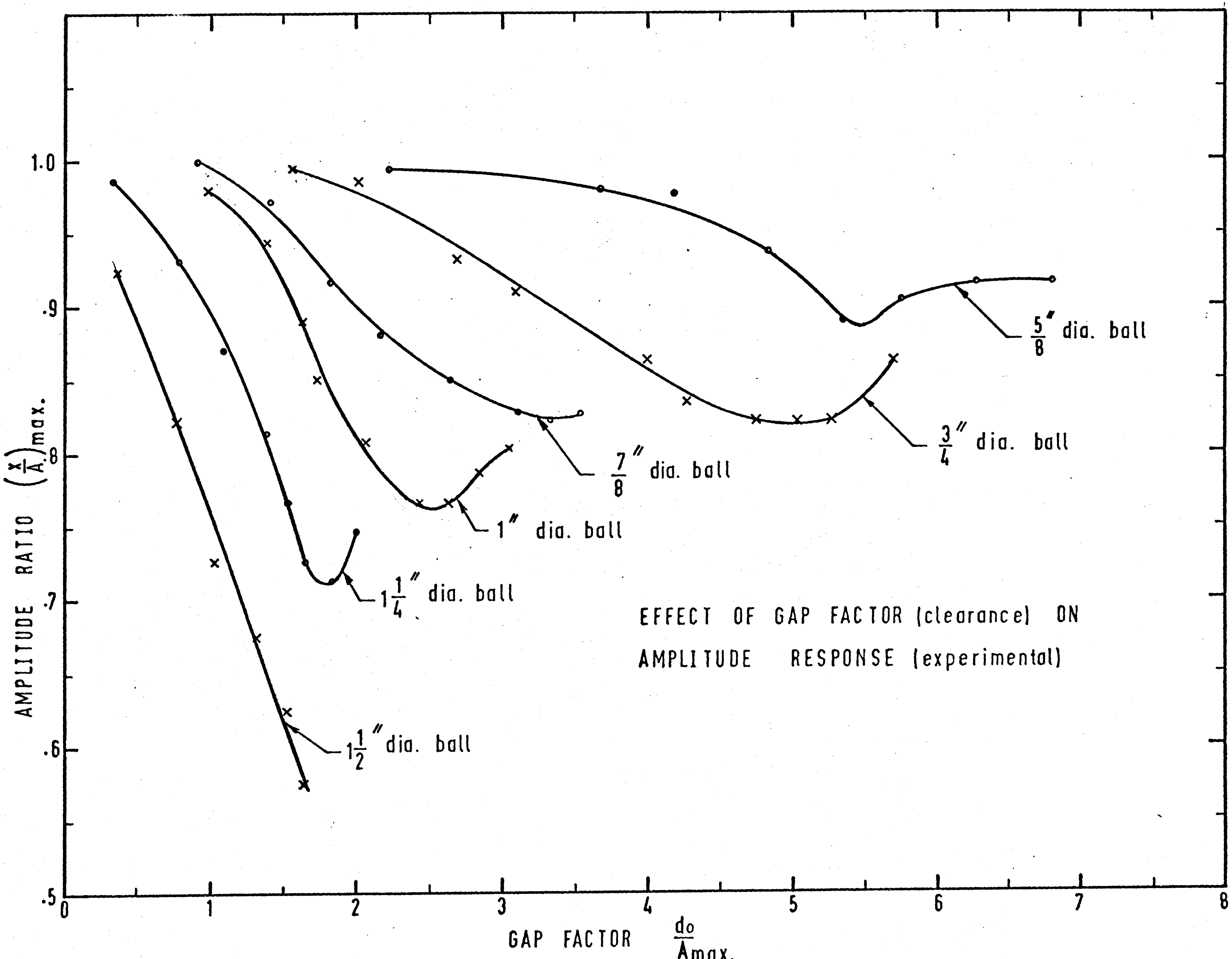

AMPLITUDE RATIO $\left(\frac{x}{A}\right)_{max.}$
GAP FACTOR $\frac{d_o}{A_{max.}}$
$\frac{5}{8}''$ dia. ball
$\frac{3}{4}''$ dia. ball
$\frac{7}{8}''$ dia. ball
$1''$ dia. ball
$1\frac{1}{4}''$ dia. ball
$1\frac{1}{2}''$ dia. ball
EFFECT OF GAP FACTOR (clearance) ON
AMPLITUDE RESPONSE (experimental)
1.0
.9
.8
.7
.6
.5
0
1
2
3
4
5
6
7
8

Fig. 12

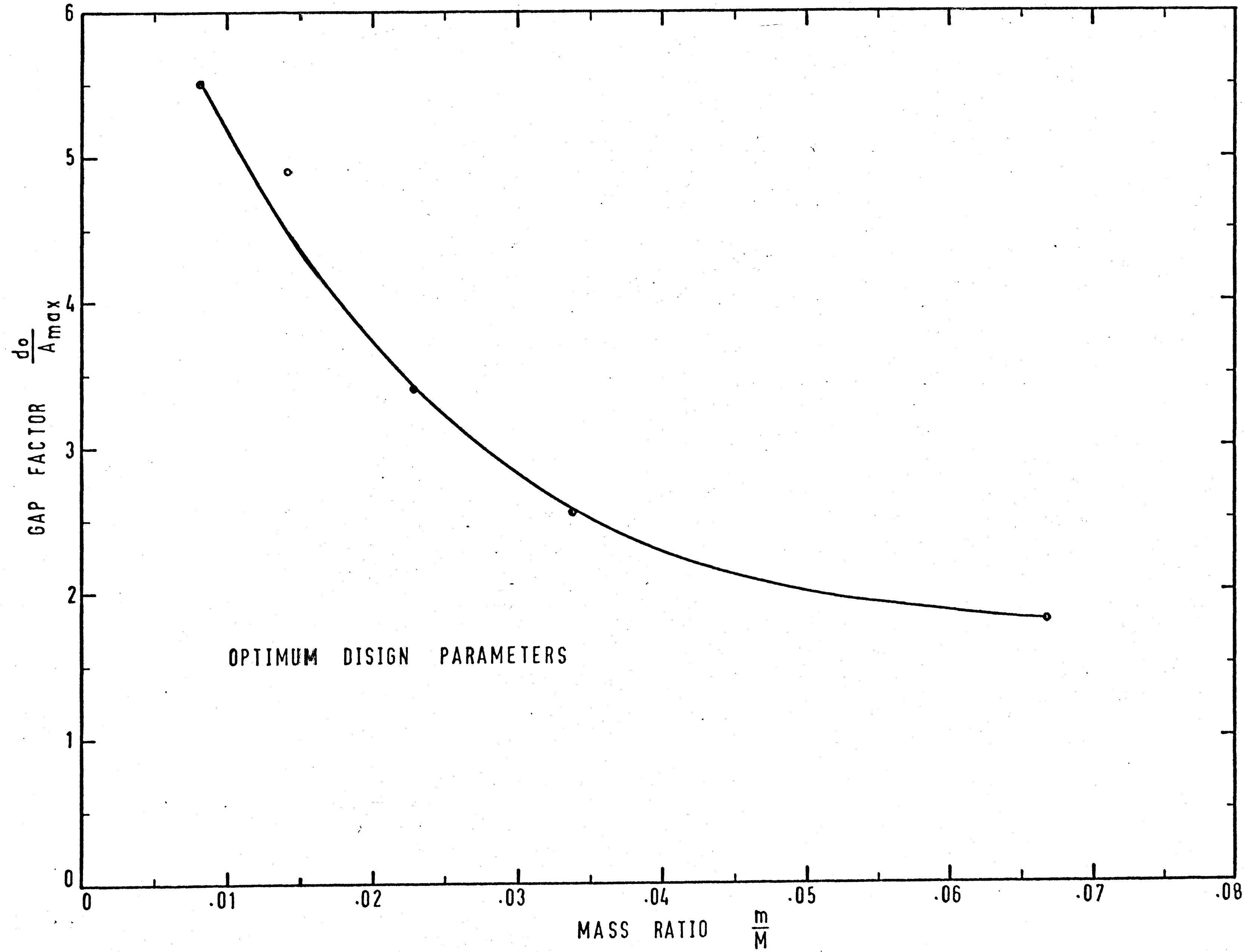
OPTIMUM DISIGN PARAMETERS
GAP FACTOR $\frac{d_o}{A_{max}}$
MASS RATIO $\frac{m}{M}$
0
1
2
3
4
5
6
0
.01
.02
.03
.04
.05
.06
.07
.08

Fig. 12.1

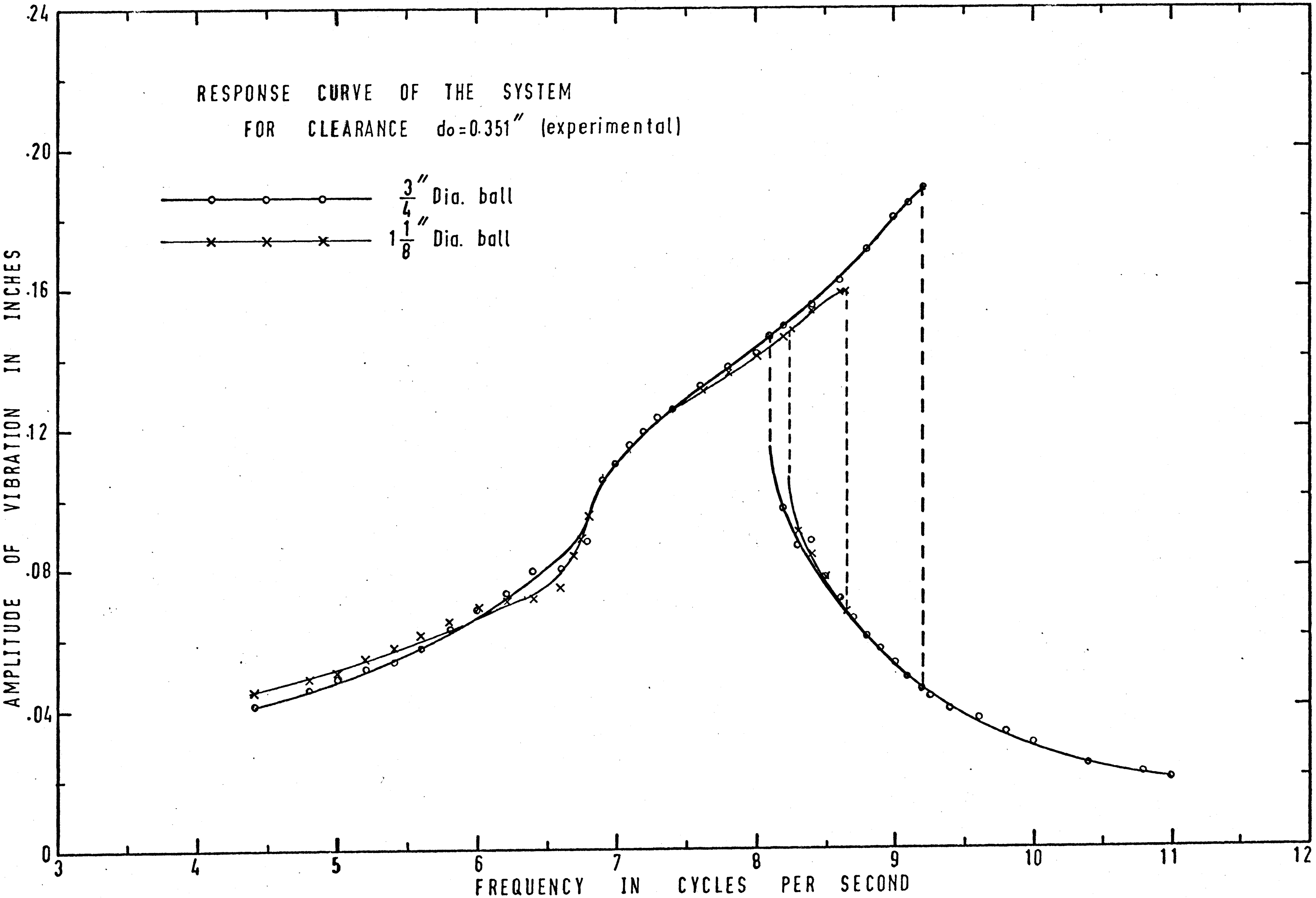
RESPONSE CURVE OF THE SYSTEM
FOR CLEARANCE do=0.351″ (experimental)
3/4″ Dia. ball
1 1/8″ Dia. ball
AMPLITUDE OF VIBRATION IN INCHES
.24
.20
.16
.12
.08
.04
0
3
4
5
6
7
8
9
10
11
12
FREQUENCY IN CYCLES PER SECOND
Fig. 13

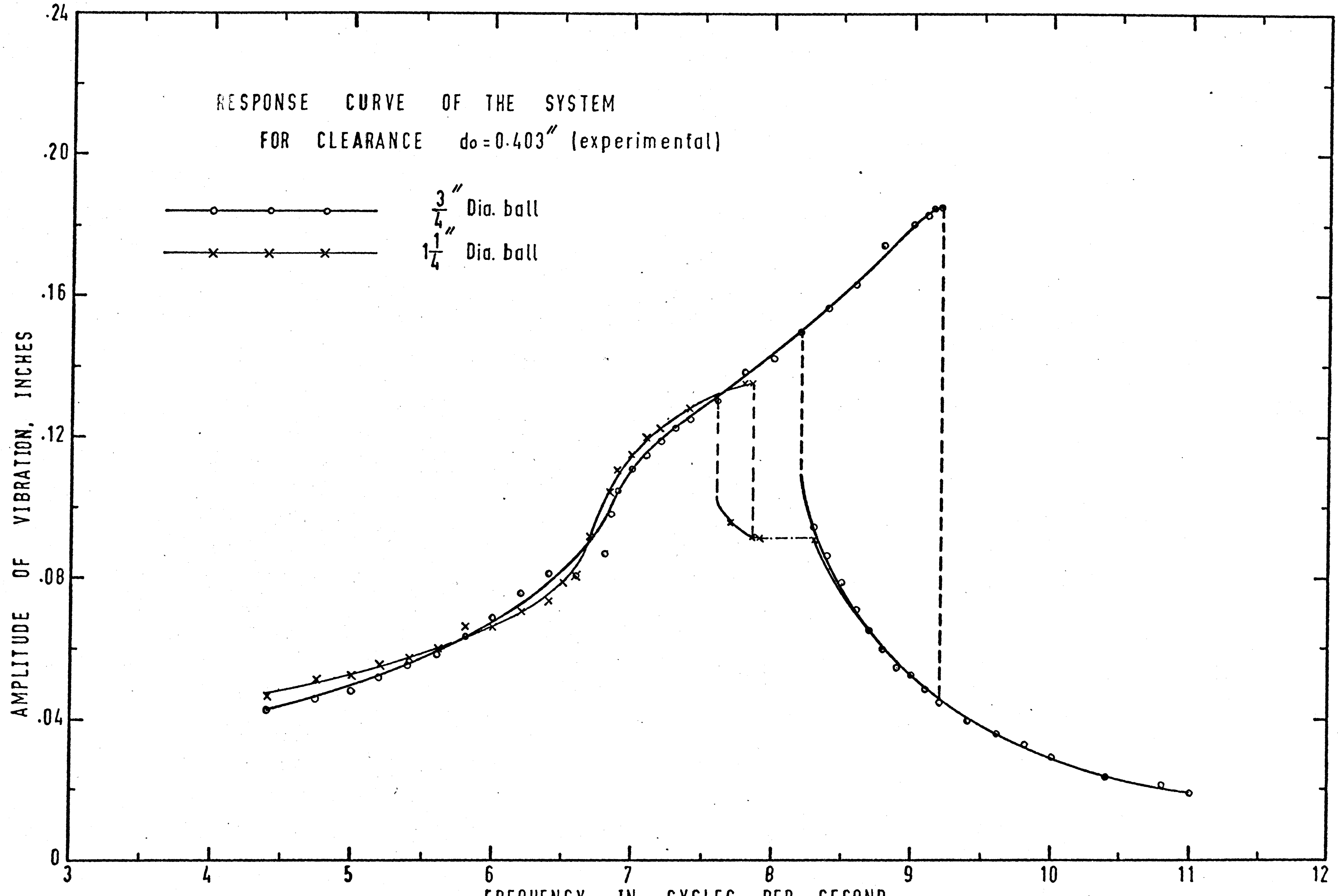
RESPONSE CURVE OF THE SYSTEM
FOR CLEARANCE do = 0.403" (experimental)
3/4" Dia. ball
1 1/4" Dia. ball
AMPLITUDE OF VIBRATION, INCHES
.24
.20
.16
.12
.08
.04
0
3
4
5
6
7
8
9
10
11
12
FREQUENCY IN CYCLES PER SECOND

Fig. 14

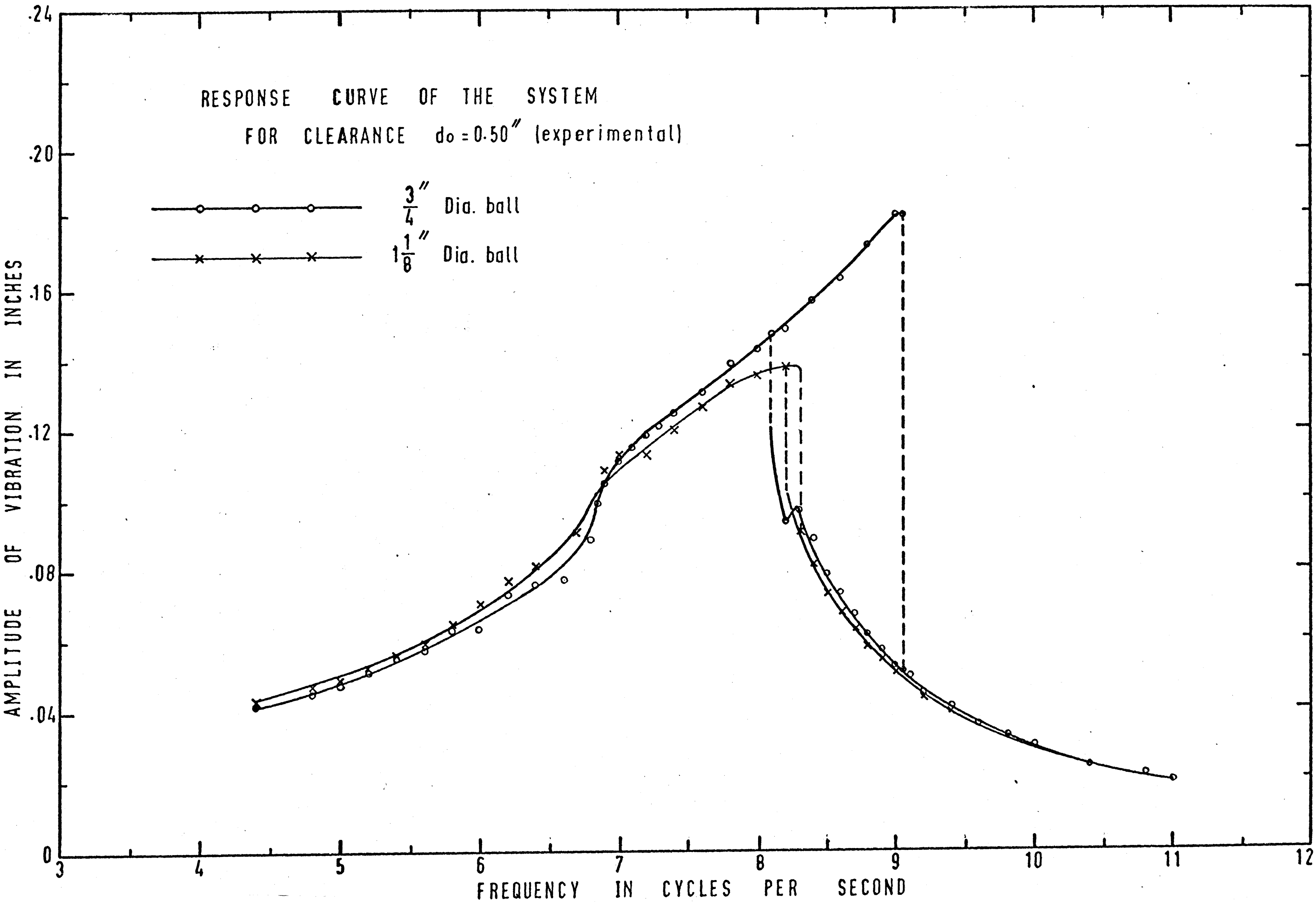
RESPONSE CURVE OF THE SYSTEM
FOR CLEARANCE do = 0.50″ (experimental)
3/4″ Dia. ball
1 1/8″ Dia. ball
AMPLITUDE OF VIBRATION IN INCHES
FREQUENCY IN CYCLES PER SECOND
.24
.20
.16
.12
.08
.04
0
3
4
5
6
7
8
9
10
11
12

Fig. 15

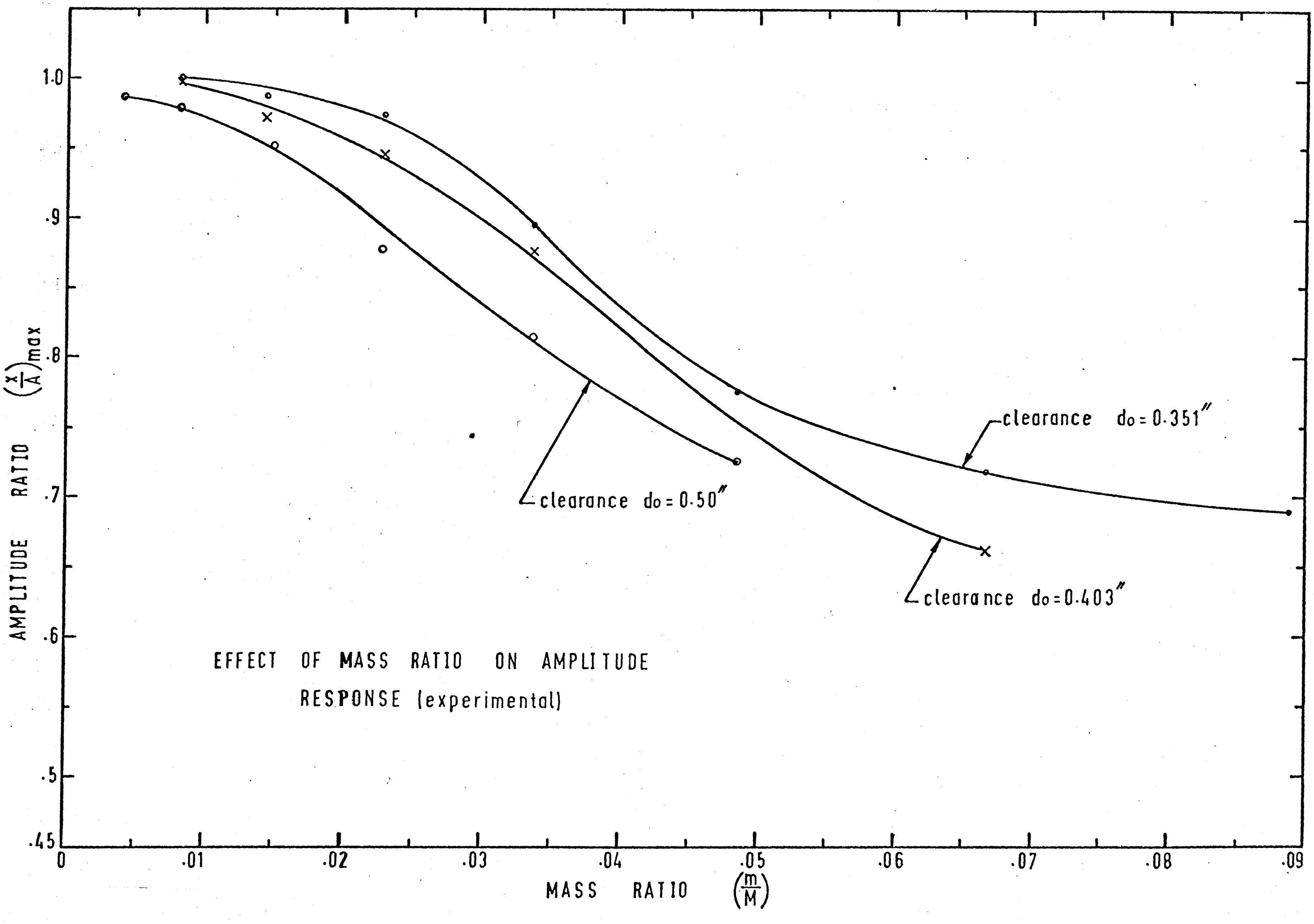

1.0
.9
.8
.7
.6
.5
.45
AMPLITUDE RATIO $\left(\frac{x}{A}\right)_{max}$
0
.01
.02
.03
.04
.05
.06
.07
.08
.09
MASS RATIO $\left(\frac{m}{M}\right)$
clearance $d_o = 0.351''$
clearance $d_o = 0.50''$
clearance $d_o = 0.403''$
EFFECT OF MASS RATIO ON AMPLITUDE
RESPONSE (experimental)

Fig.16

3. THEORETICAL STUDIES

3.1 Steady State Motion of the Primary System Without Impact Vibration Absorber

Steady state motion of such a system has been obtained in Appendix I (eqns. (I.7) and (I.24). This is given by

$$x = A \sin (\omega t - \psi) \tag{3.1}$$

where A and ψ can be evaluated from

$$\left[\frac{K_2}{K_1} + \frac{2}{\pi}\left(\frac{K_1 - K_2}{K_1}\right)\left(\left(\frac{X_1}{A}\right)\sqrt{1-\left(\frac{X_1}{A}\right)^2} + \sin^{-1}\left(\frac{X_1}{A}\right)\right) - \frac{\omega^2}{p_1^2}\right]^2 + \frac{4\, d^2\, \omega^2}{p_1^2}$$

$$= \left[\frac{F}{K_1 A}\right]^2 \tag{3.2}$$

and

$$\tan \psi = \frac{\dfrac{2\, d\, \omega}{p_1}}{\dfrac{K_2}{K_1} + \dfrac{2}{\pi}\left(\dfrac{K_1 - K_2}{K_1}\right)\left[\left(\dfrac{X_1}{A}\right)\sqrt{1-\left(\dfrac{X_1}{A}\right)^2} + \sin^{-1}\left(\dfrac{X_1}{A}\right)\right] - \dfrac{\omega^2}{p_1^2}} \tag{3.3}$$

respectively.

The values of A and ψ for different excitation frequency ω and known parameters (viz. K_1, K_2, X_1, p_1, d and F) were calculated and is tabulated in Appendix V, (Table V.1) (see programme - 1 in Appendix - X).

Amplitude response of the system with varying frequency is plotted in Figure 5 (labelled theoretical). On the same graph corresponding experimental results have also been plotted for comparison purposes. It should be noted here, that the value of 'd' (i.e. damping factor) as determined experimentally from the time history of free vibration of the system was found to be equal to 0.01854. With this value of d resonance amplitude of the system (shown in Figure 5 labelled theoretical - d = 0.01854) was infinite and asymptotic to the backbone curve. But since the structural damping increases with amplitude of vibration, experimentally determined 'd' (which was carried out for small amplitude of vibration), did not give correct information. For this reason a more widely used value of 'd' (= 0.045) for structural damping was used. And the amplitude response curve of the system using this value of 'd' is shown in Figure 5 (labelled theoretical - d = 0.045).

3.2 Resulting Motion of the Primary System With Impact Vibration Absorber

In Appendix II, it has been shown that the motion of mass M and m during the time interval from t_{i_+} (i.e. the time immediately after i^{th} impact) to the time immediately preceding next impact $t_{(i+1)_-}$ can be described by

$$x = A \sin(\omega t - \psi)$$

$$y = -x + (x_i + y_i) + (\dot{x}_i + \dot{y}_i)(t - t_i) \tag{3.4}$$

where

$$t_{i_+} < t < t_{(i+1)_-}$$

and the following relationships which were obtained from impact conditions:

$$x(t_{(i+1)_+}) = x(t_{(i+1)_-})$$

$$y(t_{(i+1)_+}) = y(t_{(i+1)_-}) \; ; \; |y| = \frac{d_o}{2}$$

$$\dot{x}(t_{(i+1)_+}) = \dot{x}(t_{(i+1)_-}) + \left[\mu\frac{(1+e)}{1+\mu}\right] \dot{y}(t_{(i+1)_-}) \qquad (3.5)$$

$$\dot{y}(t_{(i+1)_+}) = -e\,\dot{y}(t_{(i+1)_-})$$

can be used in eqn. (3.4) as new initial conditions in the time domain from $t_{(i+1)_+}$ to $t_{(i+2)_-}$. This process, when repeated over and over again, would give time behaviour of the system.

A digital computer programme to find the 'exact' sequence of the initial conditions from (3.5) and the resulting motion of the system according to (3.4) for any given set of parameters and "initial" initial conditions was written in FORTRAN IV language and was executed by an I.B.M. 7040 digital computer at the Computing and Data Processing Centre of McMaster University (see programme - 2 and 3 in Appendix X).

Among the basic features of the programme, the following ones are worth mentioning.

a) The right hand side of equation (3.4) was evaluated for $t = t_i + (K-1)/100$ (Initial values of t_i and K were taken to be zero and 2 respectively) with K increasing by 1 each time until the quantity $(\frac{d_o}{2} - |y|)$ became negative.

b) When condition (a) was satisfied, then starting with this value of t, Newton-Raphson[13] method was applied to find $t_{(i+1)}$ for which

$$\left|\frac{\frac{d_o}{2} - |y|}{d_o}\right| \leqslant 10^{-6} \quad .$$

With this value of t for which condition (b) was satisfied (which consequently represents the time at which impact took place), x, y (from eqn. (3.4)); $\dot{x}$ (from $\dot{x} = \omega A \cos(\omega t - \psi)$), and $\dot{y}$ (from $\dot{y} = -\dot{x} + \dot{y}_i + \dot{x}_i$, eqn. (II.14))were evaluated and, substituting these in the right hand side of eqns. (3.5), new initial conditions were obtained. With these new initial conditions the cyclic process was repeated again. On repeating this cyclic process over and over again, a time behaviour of the system was obtained. A typical digital computer output is shown in Table V.2, in Appendix V.

In Figures 17, 18 and 19, theoretical amplitude response curves of the system with and without an absorber have been drawn. In Figure 18, a corresponding experimental curve of the system (with absorber) has also been superimposed.

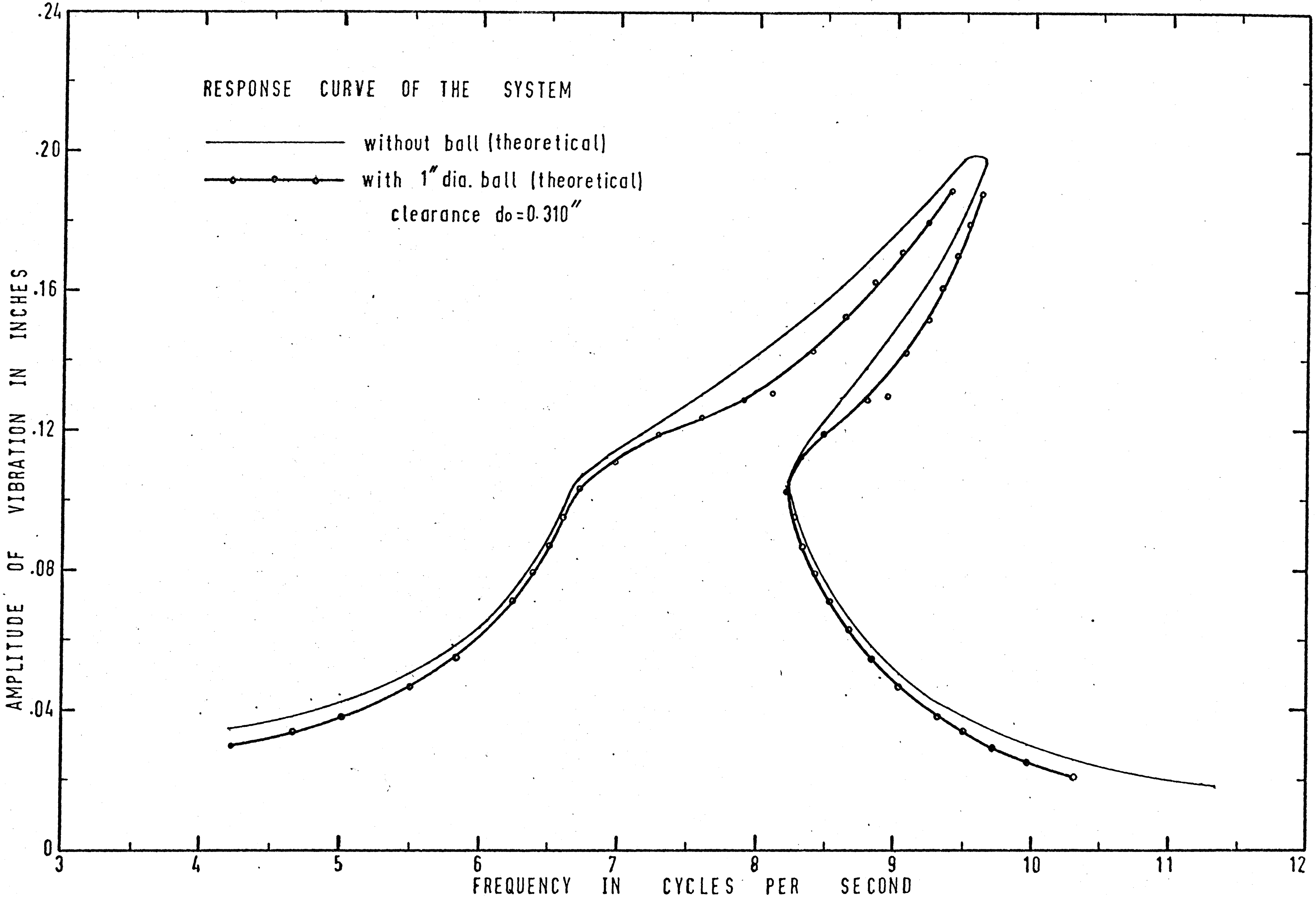
RESPONSE CURVE OF THE SYSTEM
without ball (theoretical)
with 1" dia. ball (theoretical)
clearance do=0.310"
AMPLITUDE OF VIBRATION IN INCHES
.24
.20
.16
.12
.08
.04
0
3
4
5
6
7
8
9
10
11
12
FREQUENCY IN CYCLES PER SECOND

Fig. 17

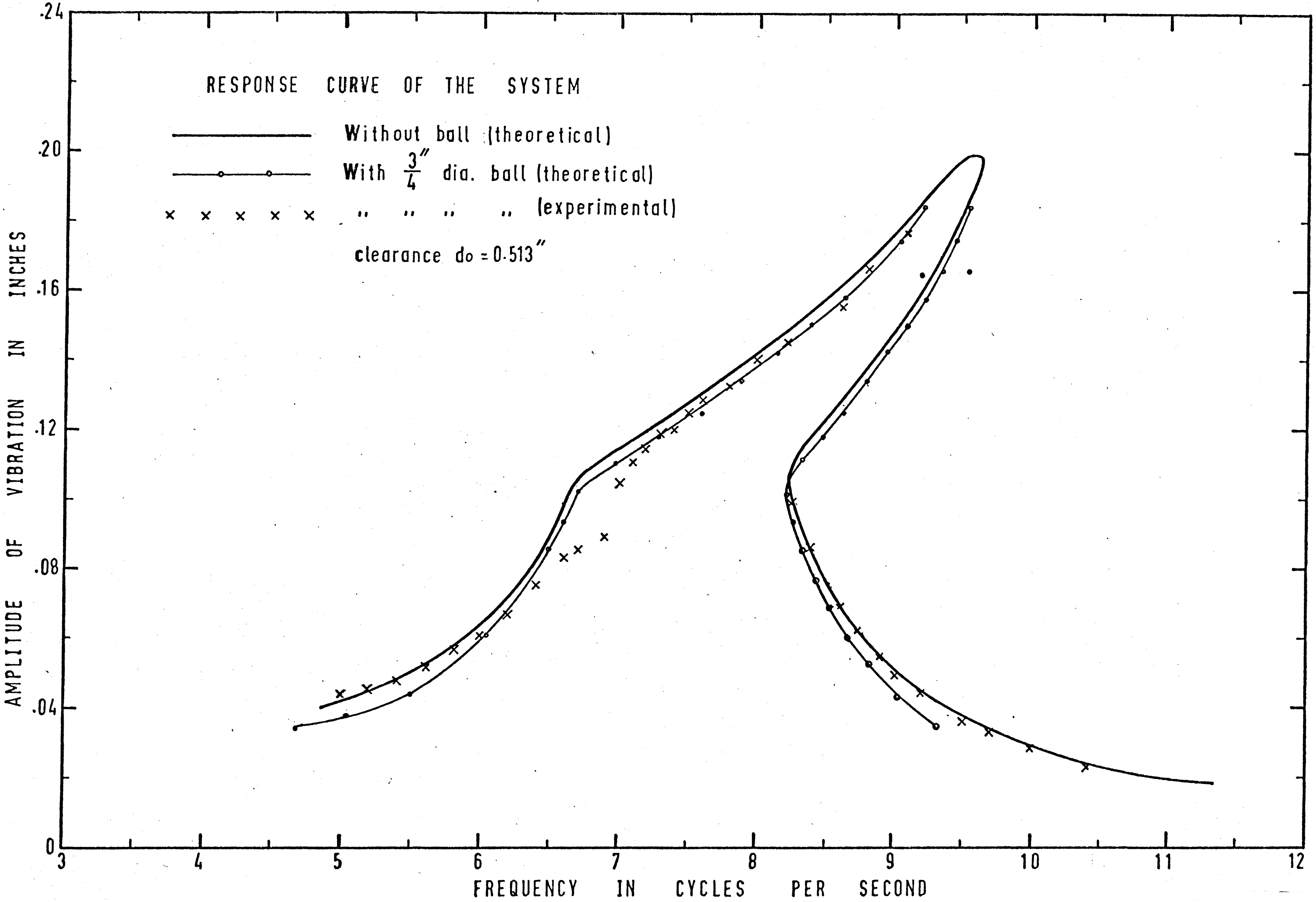
RESPONSE CURVE OF THE SYSTEM
Without ball (theoretical)
With $\frac{3}{4}''$ dia. ball (theoretical)
" " " " (experimental)
clearance do = 0.513"
AMPLITUDE OF VIBRATION IN INCHES
FREQUENCY IN CYCLES PER SECOND
.24
.20
.16
.12
.08
.04
0
3
4
5
6
7
8
9
10
11
12

Fig. 18

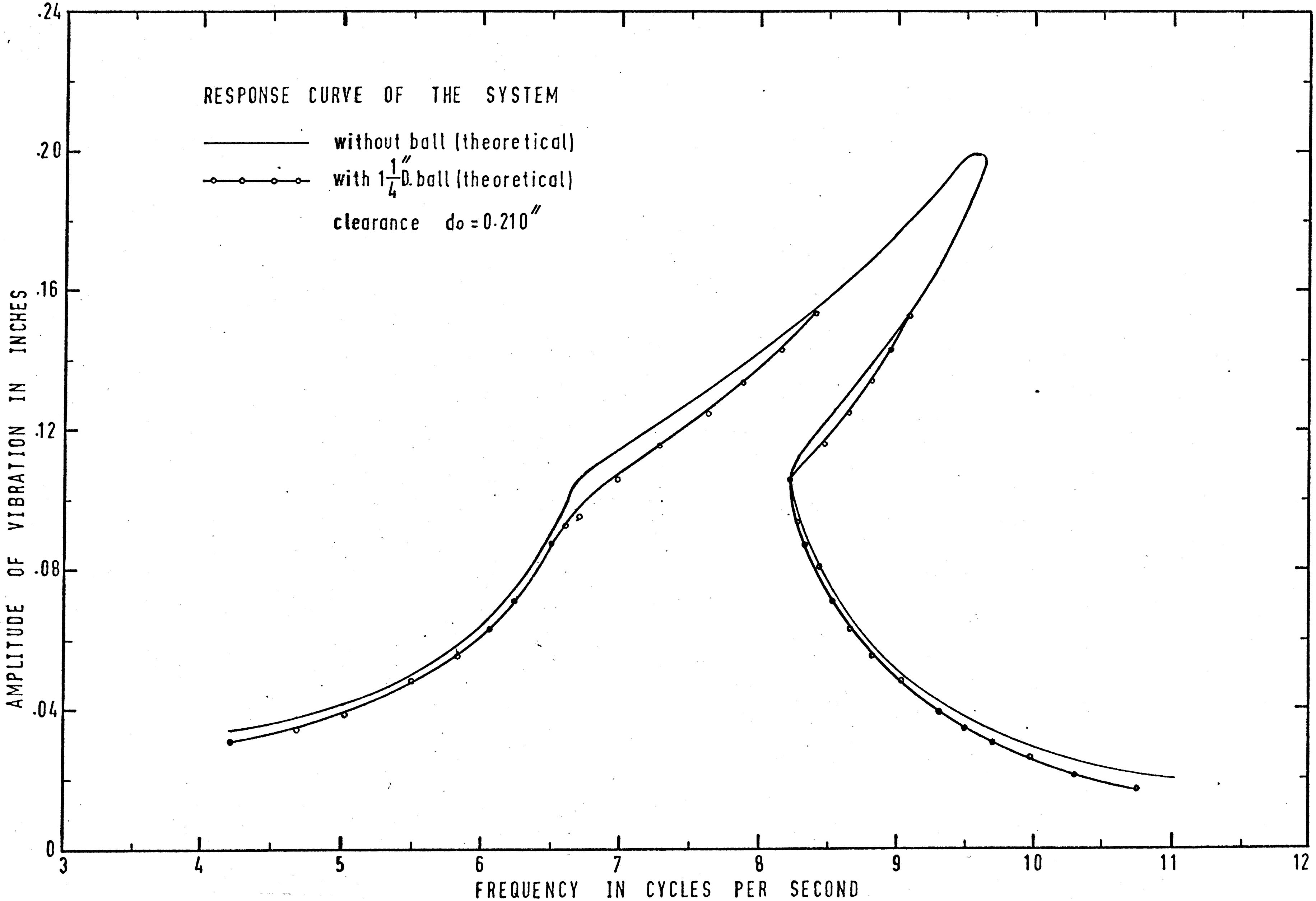
RESPONSE CURVE OF THE SYSTEM
without ball (theoretical)
with $1\frac{1}{4}''$ D. ball (theoretical)
clearance $d_o = 0{\cdot}210''$
AMPLITUDE OF VIBRATION IN INCHES
FREQUENCY IN CYCLES PER SECOND
0
.04
.08
.12
.16
.20
.24
3
4
5
6
7
8
9
10
11
12

Fig. 19

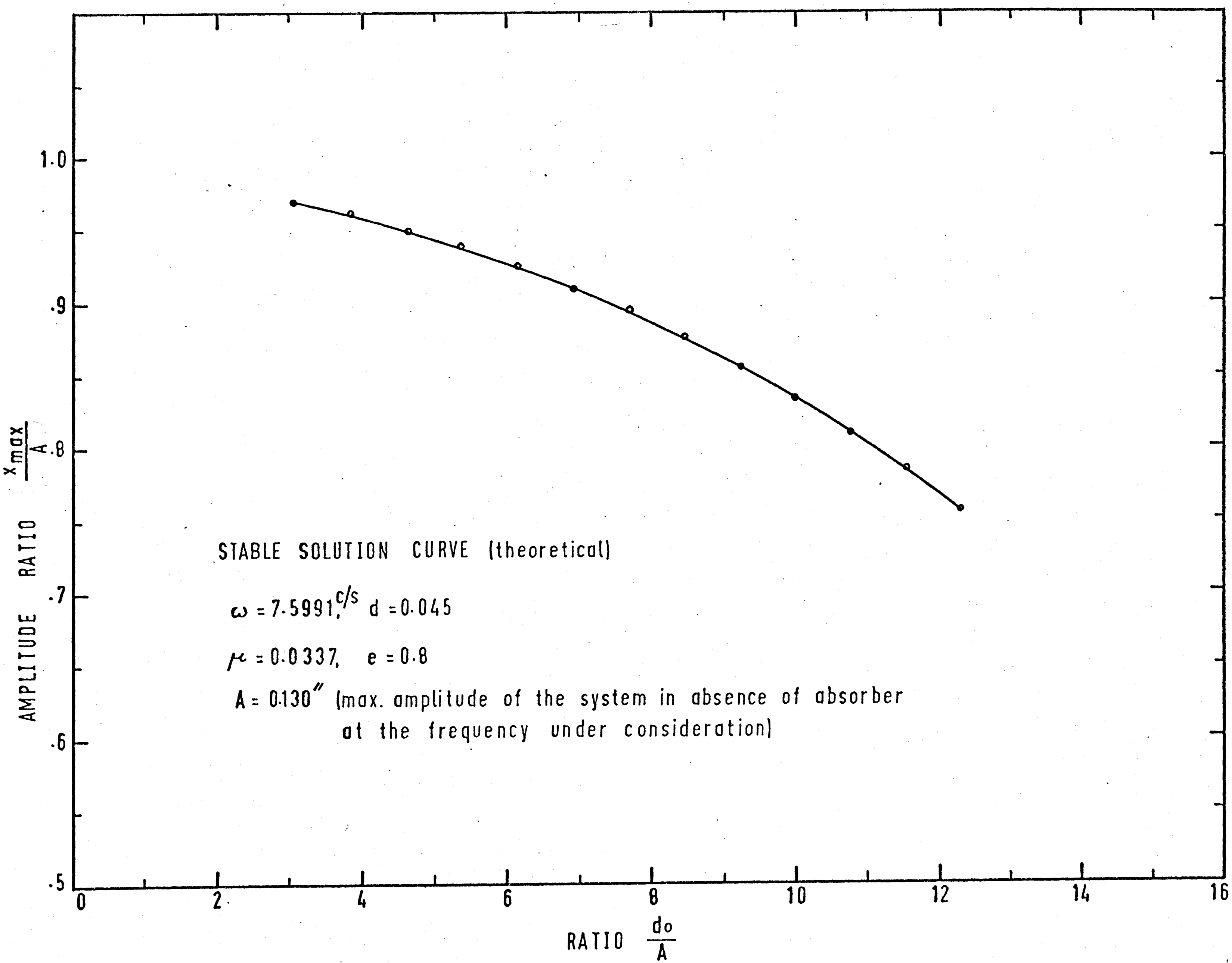

1.0
.9
.8
.7
.6
.5
0
2
4
6
8
10
12
14
16
AMPLITUDE RATIO $\frac{x_{max}}{A}$
RATIO $\frac{do}{A}$
STABLE SOLUTION CURVE (theoretical)
ω = 7.5991 c/s, d = 0.045
μ = 0.0337, e = 0.8
A = 0.130″ (max. amplitude of the system in absence of absorber at the frequency under consideration)

Fig. 20

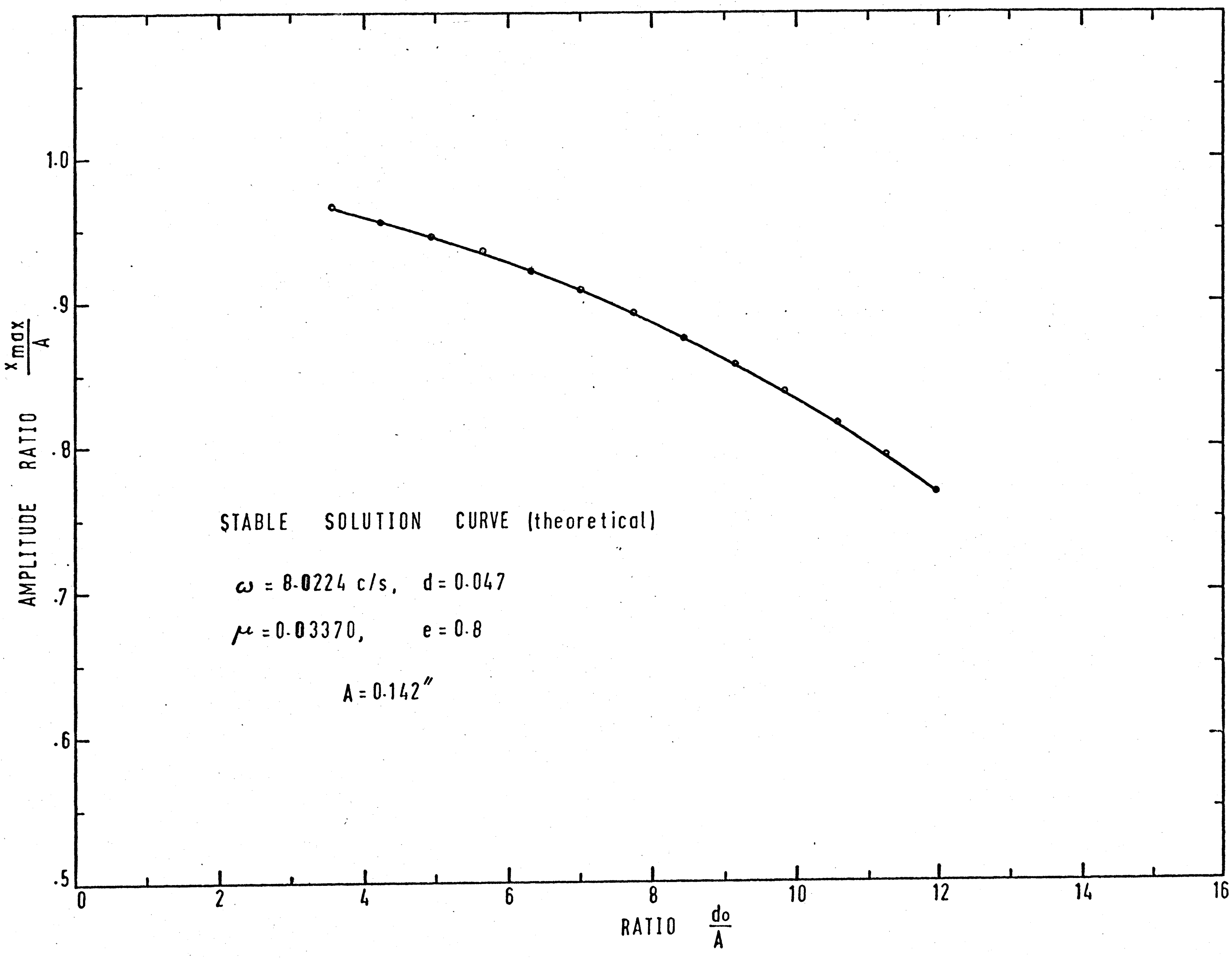
STABLE SOLUTION CURVE (theoretical)
ω = 8·0224 c/s, d = 0·047
μ = 0·03370, e = 0·8
A = 0·142″
AMPLITUDE RATIO $\frac{x_{max}}{A}$
RATIO $\frac{d_o}{A}$
1.0
.9
.8
.7
.6
.5
0
2
4
6
8
10
12
14
16

Fig. 21

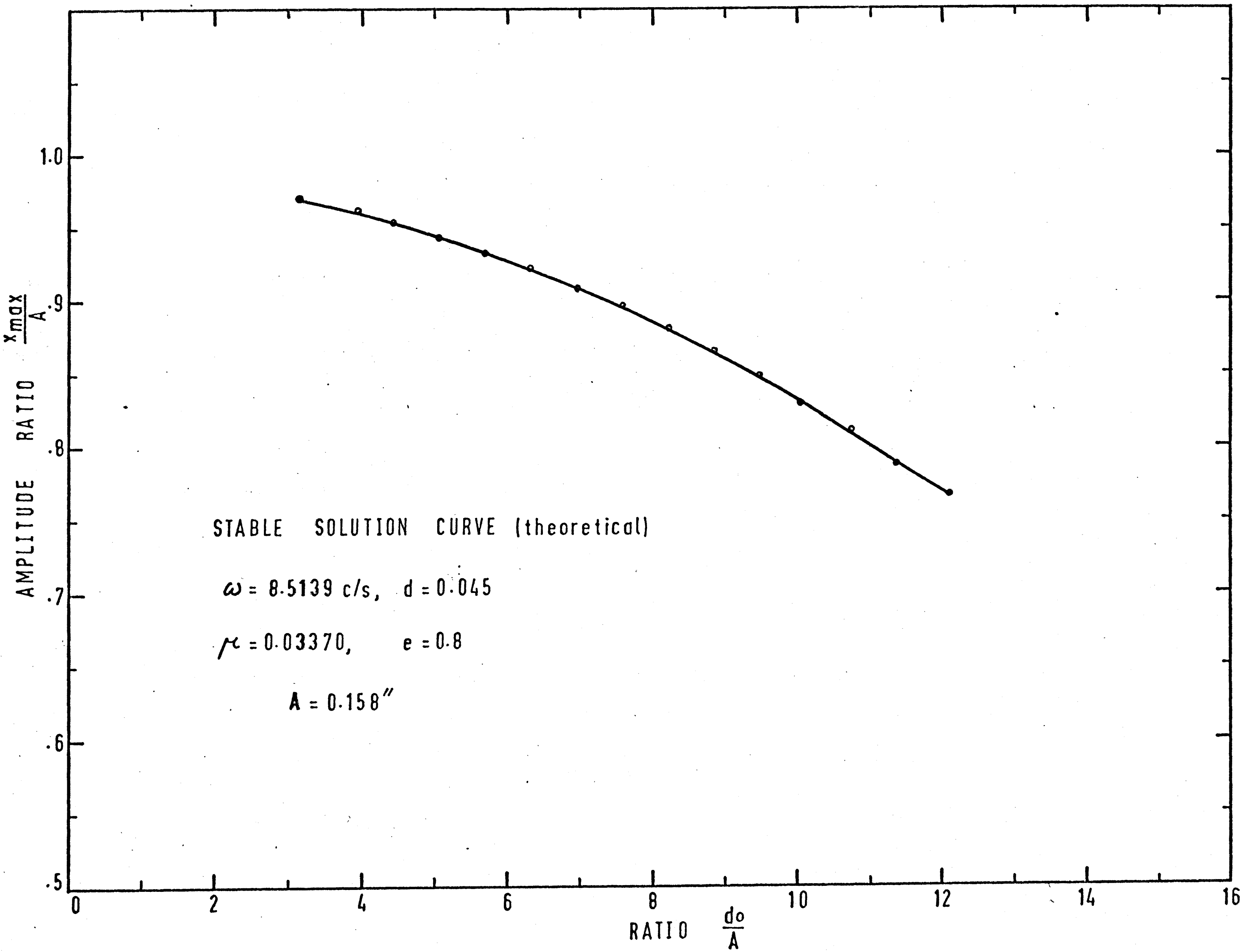

AMPLITUDE RATIO $\frac{x_{max}}{A}$
1.0
.9
.8
.7
.6
.5
0
2
4
6
8
10
12
14
16
RATIO $\frac{do}{A}$
STABLE SOLUTION CURVE (theoretical)
ω = 8.5139 c/s, d = 0.045
μ = 0.03370, e = 0.8
A = 0.158″

Fig. 22

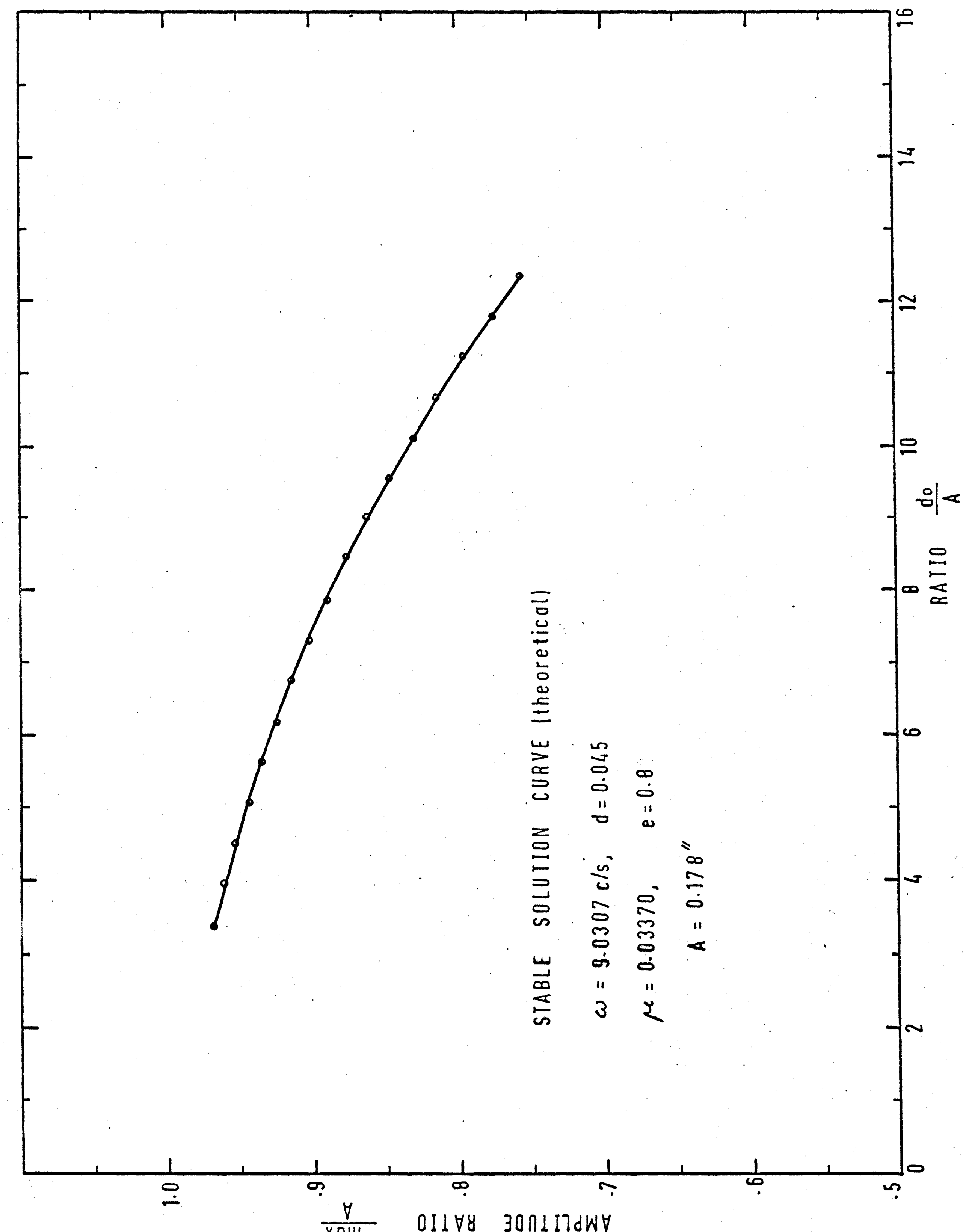
STABLE SOLUTION CURVE (theoretical)
ω = 9.0307 c/s, d = 0.045
μ = 0.03370, e = 0.8
A = 0.178″
AMPLITUDE RATIO $\frac{x_{max}}{A}$
RATIO $\frac{d_o}{A}$
1.0
.9
.8
.7
.6
.5
0
2
4
6
8
10
12
14
16

Fig. 23

4. DISCUSSION AND CONCLUSION

4.1 Discussion of Results

If amplitude response curves of an undamped non-linear system with different excitation parameter be drawn, then, from stability analysis of the system, it can be shown that the region bounded by the backbone curve (i.e. the curve corresponding to zero excitation) and the loci of points at which the response curves (for different excitation parameters) have vertical tangent is unstable. For a damped non-linear system the unstable region is bounded by the locus of vertical tangents to the families of constant excitation curves.

In Figure 5, from the experimental response curve of the system (which corresponds to a constant excitation parameter) it can be seen that during frequency increase the amplitude became as large as 0.1906" at $\omega = 9.5$ c/s and almost at the same frequency it suddenly dropped down to 0.035" and went on decreasing as excitation frequency was increased. On reversing the process from this region (i.e. in decreasing ω slowly), amplitude started growing up slowly until it reached about 0.106" at $\omega = 8.2$ c/s and then it suddenly went up to 0.136" at the same ω. This sudden fall and rise in amplitude (at the same frequency) is known as the 'jump phenomenon' and is associated with a non-linear systems and this occurs when response curve corresponding to a certain excitation parameter approaches the unstable boundary. If the system under consideration operates in any of the stable regions bounded by two imaginary vertical lines through the dotted ones, in Figure 5, a very small accedental unsteadiness or extraneous disturbance may readily bring the system over the instability threshold into the unstable region and ultimately to a stable region, other than the one in which it initially was.

In Figure 5, the experimental curve drawn in conjunction with the theoretical one shows a good agreement between theory and experiment.

In Figures 6 - 11, experimental amplitude response curves of the system provided with an impact vibration absorber have been plotted. Each one of these figures contains about 3 curves and each of them represents the system response for one parameter variation of the absorber namely gap factor.

From these graphs one can obtain the information regarding, if introduction of an absorber has any effect on resulting motion of the system, whether the introduction of such a thing results in an increase or decrease in the resulting motion and, if any, what effect one might expect if one of the parameters (gap factor in this case) of the absorber is changed.

For instance, in Figure 6 where the amplitude response of the system provided with an absorber (having 5/8" dia. ball) has been plotted, shows that the maximum amplitude for the system for d_o = .423" was .1893" and for d_o = 1.019" was .1698" in comparison to .1906" with no absorber. It should, however, be noted that although the absorber with d_o = 1.019" reduced the maximum amplitude to a greater extent in comparison to the one having d_o = .423", the later one (d_o = 1.019") is less efficient below $\omega = 7$ c/s, because due to bigger length of travel the absorber did not come into operation until the primary amplitude of the system reached a certain value.

The small humps in the response curves as seen in Figures 8, 9 and 10 are the result of the impact vibration abosrber's sudden coming into operation associated with reduction in amplitude.

Figure 12, in which the maximum amplitude ratio against gap factor has been plotted, shows the effect of gap factor on maximum amplitude of vibration of the system. It is seen that with a particular absorber an increase in gap factor from its lowest value was accompanied by a decrease in amplitude ratio of the system at first until a certain optimum value was reached, after which an increase in gap factor resulted in an increase in amplitude ratio. For instance, with 3/4" dia. ball absorber an optimum value of amplitude ratio = .82 was obtained for a gap factor = 5. Any increase or decrease in gap factor from this value resulted in an increase in amplitude ratio. For 1 1/2" dia. ball no optimum value was reached. From these curves it is also seen that the bigger the mass of the absorber the more effective is the device. This point will be raised again when the effect of mass ratio will be investigated.

The experimental points on extreme right hand of these curves represent the points up to which the system was stable (stable in the sense that the motion of the ball was regular). Any further increase in gap factor resulted in an irregular motion of the ball and amplitude did not remain constant.

Figure 12.1 gives information regarding the choice of parameters for optimum design of the system. Figures 13 - 15 give information regarding the effect of absorber mass on the resulting motion of the system. In these figures it is seen that at low excitation frequency amplitude of vibration of the system with an absorber of bigger mass was larger than that with the one of lower mass having the same clearance. The explanation for this is that with an absorber of bigger mass the effective mass of the system increased considerably and thereby decreased the natural frequency of the system, whereas for an absorber with smaller mass the natural frequency of the system remained unaffected. Now taking a simple linear case, where motion of the system is given by

$$\left[1 - \frac{\omega^2}{p_1^2}\right]^2 + \frac{4\, d^2\, \omega^2}{p_1^2} = \left[\frac{F}{K_1 A}\right]^2$$

where p_1 is the natural frequency of the system, it can be shown that if A is the amplitude of vibration of the system having natural frequency p_1 for a certain excitation frequency ω and A' is the amplitude of a system having slightly different natural frequency p_1' at the same ω, where $p_1' < p_1$, then $A' > A$ for $\omega < p_1$ and $A' < A$ for $\omega > p_1$. Thus it is obvious that unless the effect of impact nullify this effect then introduction of an absorber with a bigger mass would be of no advantage at low frequency range. But it is seen that with an absorber of a bigger mass maximum amplitude attained by the system is less than that attained with an absorber of lower mass. The discontinuous horizontal line in Figure 14 indicates unstable region.

Figure 16 shows the effect of mass ratio between the absorber and the primary mass on the maximum amplitude attained by the system. These show that an increase in mass ratio resulted in decreasing the amplitude ratio of the system. Though the curve with clearance $d_o = 0.351''$ was approaching towards an optimum, from the present study it can not be said definitely that such an optimum mass ratio exists, since the investigation was not carried out beyond the extreme right hand point for this case, and for other cases viz. with $d_o = 0.403''$ and $0.50''$ further increased in mass ratio resulted in an unstable motion.

If a horizontal line is drawn through these curves then the intersection points would give the design parameters for three different absorber systems which will produce the same amplitude reduction of the system. For instance each of the following absorbers having different parameters (1) $\mu = 0.0555$, $d_o = 0.351''$ (2) $\mu = 0.04925$, $d_o = 0.403''$ (3) $\mu = 0.0435$, $d_o = 0.50''$ would give a maximum amplitude ratio of 0.75.

Figures 17 - 19 show theoretical response curves (obtained numerically by direct step by step construction of the time behaviour of the system) of the system with an absorber in conjunction with the one with no absorber. In Figure 18, the corresponding experimental curve has also been superimposed, from which it is observed that the agreement between theory and experiment is good. The discrepancy which is seen in the amplitude range from .08" to .11" might have arisen due to some misalignment in the guide block which introduced non-linearity in the cantilever type leaf springs during the course of investigation (it may be recalled here that initially the model was so adjusted that the stiffness K_2 came into play when X_1 was equal to .104").

It should be mentioned here that with an absorber having 1" dia.

ball and clearance d_o = 0.310", maximum amplitude attained by the system as given by experiment was 0.1696", while with the same absorber theoretically obtained stable (stable in the sense that symmetric 2 impacts per cycle motion existed) maximum amplitude was only 0.1302" at ω = 7.8866 c/s. However, unsymmetric but stable maximum amplitude recorded was as high as .189", or more precisely an oscillating value between .179" and .189".

In Figure 19, theoretical behaviour of the system with an absorber having 1 1/4" dia. ball and clearance d_o = .210" has been shown. Experimentally the system was found to be stable throughout the frequency range under consideration and the maximum amplitude attained by the system was .1657". Theoretical results predicted that symmetric 2 impacts per cycle stable motion was possible until the amplitude of the system became 0.0935", after which unsymmetric but regular motion became predominant and such a motion maintained until the maximum amplitude reached was 0.153". After this the motion became irregular and gave no consistent record of amplitude.

In Figures 20, 21, 22 and 23 theoretically obtained amplitude ratio $\frac{x_{max}}{A_d}$ (see computer programme no. 4 in Appendix X) has been plotted against $\frac{o}{A}$ each for one fixed frequency. In these curves only those solutions have been plotted which predicted the stable motion of the system (stable in the sense that symmetric 2 impacts per cycle motion existed), and they have been referred as 'stable solution curve'.

These curves give information regarding the stability of the system with a particular absorber at a certain operating frequency. For instance Figure 20 predicts that if the system having mass ratio

$\mu = 0.03770$, be operated at an excitation frequency of $\omega = 7.5991$ c/s, the system will remain stable if the parameter $\frac{d_o}{A}$ (this is proportional to the clearance d_o) is kept within the range 3.077 - 12.3. In the same way Figures 21, 22 and 23 can also be interpreted.

By obtaining the stable solution curves for the entire operating frequency range (4 - 11 c/s for the present case) and for various mass ratios μ, one can obtain the stability boundaries of the system (a plot of $\frac{d_o}{A}$ against ω), which will then give ready answer to, if the system parameters chosen for a particular system would give rise to a stable motion of the system.

In the present analysis stable solution curves for only four isolated frequencies and for a single mass ratio were obtained, so no attempt had been made to construct a stability boundary curve. In reference (6) on page 72 such a curve had been drawn for a linear system.

Finally, an endeavour was made to obtain the solution of the eqns. of motion of the system by Runge-Kutta method[14]. Here, the two basic simultaneous equations of motion of the primary system and the mass particle in the absorber system were solved by the numerical method just mentioned by starting the solution with given initial conditions and then imposing new initial conditions (obtained from impact conditions) after each impact. Although this method failed to give any solution in the frequency range where multivalued solution is possible, the solutions given by this in other frequencies agreed with the one obtained by other numerical method within 5%.

4.2 Conclusion

As a result of the present investigation the following conclusions can be made.

1) An impact vibration absorber is capable of reducing the vibration level of a non-linear oscillating system, and the degree of its reduction is dependent on system parameters.

2) Usually, but not necessarily, the bigger the μ (i.e. mass ratio between the absorber mass and mass of the system whose amplitude is being reduced) the more reduction in amplitude is obtained.

3) For a system with an absorber where μ is fixed, an increase in gap factor ($\frac{d_o}{A}$) of the absorber might result in more reduction of amplitude of the system, provided that the original combination of system parameters was not an optimum one.

4) Like viscous damper, the impact vibration absorber is less effective in reducing below-resonance and above-resonance vibration levels, but is very effective in reducing vibration level of the resonance-amplitude.

5) Although for some parameters for which symmetric 2 impacts per cycle motion was not stable (as predicted by computer results), stable periodic motion with unsymmetric but regular impacts was found to exist.

6) Even for extreme cases, where no periodic motions were found to exist, the absorber was often effective in reducing vibration levels.

7) Usually the absorber is not very sensitive to slight changes in parameters.

8) Since it is the resulting amplitude rather than the stable periodic motion that is of prime interest for practical application, impact

vibration absorber fulfilled its role as a vibration absorbing device in disorganizing the orderly process of amplitude build-up.

In the present study the effectiveness of an impact vibration absorber on a non-linear system which was subjected to a sinusoidal excitation has only been investigated. Other problems of interest which warrant investigation are to determine its effectiveness on a randomly excited non-linear system and also on the same type of system which is subjected to a pulse-like excitation. The former investigation presumably would be better tackled by statistical means.

Regarding its application it offers a tempting choice in a system where a dynamic vibration absorber is practicable, because while the requirements of a tuned absorber must be met exactly, the effectiveness of an impact vibration absorber is relatively insensitive to system parameters. Installation of such a device in the structure of a television receiving antenna can reduce the vibration level caused by von Karman vortices and thus prevent fatigue failure of the structure. Helicopter vibration can also be controlled by installation of such a device.

APPENDIX - I

Equation of Motion of the Primary System Between Impacts and Its Steady State Solution

A non-linear differential equation may be represented in the form

$$M\ddot{x} + f_1(\dot{x}) + f_2(x) = f_3(t) \qquad \text{(I.1)}$$

in which the restoring force function $f_2(x)$ and the damping force function $f_1(\dot{x})$ are non-linear odd functions of the displacement and of the velocity, respectively. In other words, $-f_2(x) = f_2(-x)$, and $-f_1(\dot{x}) = f_1(-\dot{x})$. Dividing through by M and substituting a sinusoidal force $F \sin \omega t$ for $f_3(t)$, the differential equation becomes

$$E[\ddot{x}] = \ddot{x} + \frac{1}{M} f_1(\dot{x}) + \frac{1}{M} f_2'(x) - \frac{1}{M} F \sin \omega t = o \qquad \text{(I.2)}$$

An approximate solution of (I.2) can be assumed consisting of n appropriate terms and denoting it by $\tilde{x}$, it can be represented by

$$\tilde{x} = a_1 \phi_1(t) + a_2 \phi_2(t) + \ldots\ldots + a_n \phi_n(t) \qquad \text{(I.3)}$$

In this case, $E[\tilde{x}]$ will be different from $E[x]$, and therefore $E[\tilde{x}]$ will be different from zero. Since $\tilde{x}$ is not an exact solution $E[\tilde{x}]$ will vary from instant to instant, but over an arbitrary duration of time T it will be possible to demand that each of n weighted averages of the expression $E[\tilde{x}]$ must vanish. In mathematical language this means that

$$\int_0^T E[\tilde{x}]\ \phi_1(t)\ dt = 0, \int_0^T E[\tilde{x}]\ \phi_2(t)\ dt = 0,$$

$$\int_0^T E[\tilde{x}]\ \phi_n(t)\ dt = 0 \quad (I.4)$$

This will yield n algebraic equations from which the coefficients $a_1, a_2 \ldots, a_n$ can be found and under these circumstances the approximate solution for $\tilde{x}$ will be the best obtainable in the n term chosen. This process is known as Ritz averaging criteria[11].

In order to solve the differential equation (I.2), the Ritz averaging criteria may be expressed for the duration $T = \frac{2\pi}{\omega}$, or equally well for the angle of 2π radians, as follows,

$$\int_0^{2\pi} E[\tilde{x}]\ \cos \omega t\ d(\omega t) = 0 \quad (I.5)$$

$$\int_0^{2\pi} E[\tilde{x}]\ \sin \omega t\ d(\omega t) = 0 \quad (I.6)$$

Now let us assume a two-term approximation for x in the solution of (I.2), that is

$$\tilde{x} = A \sin (\omega t - \psi) \quad (I.7)$$

hence,

$$\dot{\tilde{x}} = \omega A \cos (\omega t - \psi) \quad (I.8)$$

and,

$$\ddot{\tilde{x}} = -\omega^2 A \sin (\omega t - \psi) \quad (I.9)$$

Substituting the approximation (I.7), and hence (I.2) into (I.5) yields

$$-\omega^2 A \int_0^{2\pi} \sin(\omega t - \psi) \cos \omega t \, d(\omega t)$$

$$+ \frac{1}{M} \int_0^{2\pi} f_1 [\, \omega A \cos(\omega t - \psi) \,] \cos \omega t \, d(\omega t)$$

$$+ \frac{1}{M} \int_0^{2\pi} f_2 [\, A \sin(\omega t - \dot{\psi}) \,] \cos \omega t \, d(\omega t)$$

$$- \frac{F}{M} \int_0^{2\pi} \sin \omega t \; \cos \omega t \, d(\omega t) = 0 \qquad \text{(I.10)}$$

If now a new angular variable $\sigma = \omega t - \psi$ be introduced so that $d\sigma = d(\omega t)$ and $\cos \omega t = \cos(\sigma + \psi)$, then (I.10) becomes

$$-\omega^2 A \int_0^{2\pi} \sin \sigma \cos(\sigma + \psi) \, d\sigma + \frac{1}{M} \int_0^{2\pi} f_1(\omega A \cos \sigma) \cos(\sigma + \psi) \, d\sigma$$

$$+ \frac{1}{M} \int_0^{2\pi} f_2(A \sin \sigma) \cos(\sigma + \psi) \, d\sigma - \frac{F}{M} \int_0^{2\pi} \sin \omega t \cos \omega t \, d(\omega t) = 0$$

On expansion this gives

$$-\omega^2 A \int_0^{2\pi} \sin \sigma \, (\cos \sigma \cos \psi - \sin \sigma \sin \psi) \, d\sigma$$

$$+ \frac{1}{M} \int_0^{2\pi} f_1(\omega A \cos \sigma) \, (\cos \sigma \cos \psi - \sin \sigma \sin \psi) \, d\sigma$$

$$+ \frac{1}{M} \int_0^{2\pi} f_2(A \sin \sigma)(\cos \sigma \cos \psi - \sin \sigma \sin \psi) \, d\sigma$$

$$= 0$$

On partial evaluation of integrals, the above equation results into

$$\omega^2 A \pi \sin \psi + \frac{1}{M} \cos \psi \int_0^{2\pi} f_1(\omega A \cos \sigma) \cos \sigma \, d\sigma$$

$$- \frac{1}{M} \sin \psi \int_0^{2\pi} f_2(A \sin \sigma) \sin \sigma \, d\sigma = 0$$

Rewriting this gives

$$-\omega^2 \sin \psi - \frac{1}{M} \cos \psi \; \frac{4}{\pi A} \int_0^{\frac{\pi}{2}} f_1(\omega A \cos \sigma) \cos \sigma \, d\sigma$$

$$+ \frac{1}{M} \sin \psi \; \frac{4}{\pi A} \int_0^{\frac{\pi}{2}} f_2(A \sin \sigma) \sin \sigma \, d\sigma = 0 \qquad \text{(I.11)}$$

or,

$$-\omega^2 \sin \psi - \frac{1}{M} G(A,\omega) \cos \psi + \frac{1}{M} H(A) \sin \psi = 0 \qquad \text{(I.12)}$$

where

$$G(A,\omega) = \frac{4}{\pi A} \int_0^{\frac{\pi}{2}} f_1(\omega A \cos \sigma) \cos \sigma \, d\sigma$$

$$H(A) = \frac{4}{\pi A} \int_0^{\frac{\pi}{2}} f_2(A \sin \sigma) \sin \sigma \, d\sigma \qquad \text{(I.13)}$$

Similarly substituting the approximation (I.7) in (I.6) and proceeding in the same manner as before would give

$$-\omega^2 \cos \psi + \frac{1}{M} G(A,\omega) \sin \psi + \frac{1}{M} H(A) \cos \psi = \frac{F}{MA} \qquad \text{(I.14)}$$

Rewriting (I.12) and (I.14) gives

$$\left[-\omega^2 + \frac{1}{M} H(A) \right] \sin \psi - \frac{1}{M} G(A,\omega) \cos \psi = 0 \qquad \text{(I.15)}$$

$$\left[-\omega^2 + \frac{1}{M} H(A) \right] \cos \psi + \frac{1}{M} G(A,\omega) \sin \psi = \frac{F}{MA} \qquad \text{(I.16)}$$

Squaring these two and adding gives

$$\left[\frac{1}{M}H(A) - \omega^2\right]^2 + \left(\frac{1}{M}\right)^2 G^2(A,\omega) = \left[\frac{F}{MA}\right]^2 \tag{I.17}$$

and from (I.15) an expression for tan ψ can be obtained.

$$\tan\psi = \frac{\frac{1}{M}G(A,\omega)}{\frac{1}{M}H(A)-\omega^2} \tag{I.18}$$

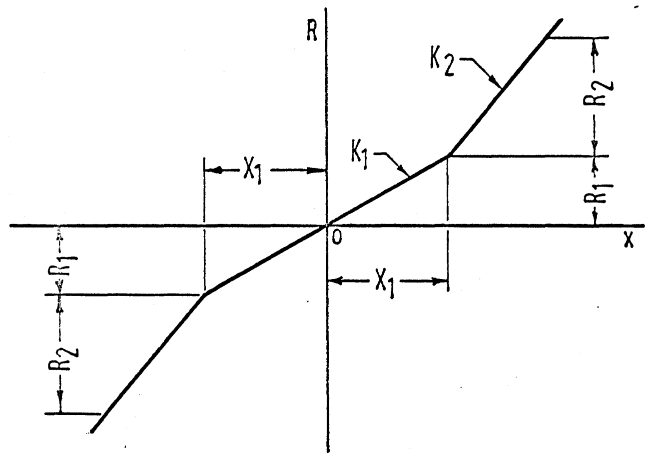

$R_1 = K_1X_1$

$R_2 = K_2(x-X_1)$

$R = (K_1-K_2)X_1+K_2x$

x = Spring extension

R = Restoring force

K_1, K_2 = Spring stiffness

Fig. I.1: Spring restoring force versus spring extension curve

From the above figure it is seen that for the problem under consideration the restoring force function $f_2(x)$ can be represented by

$$f_2(x) = K_1 x \quad \text{for} \quad o<|x|< X_1$$

and (I.19)

$$f_2(x) = (K_1-K_2)X_1 + K_2 x \quad \text{for} \quad X_1 < |x|$$

For region 1 ($o<|x| < X_1$), H(A) can be evaluated from (I.13)

$$H(A) = \frac{4}{\pi A}\int_o^{\frac{\pi}{2}} K_1(A \sin^2\sigma)\, d\sigma$$

on evaluating this integral gives

$$H(A) = K_1$$

For region 2 ($X_1 < |x|$), H(A) is evaluated as follows:

$$H(A) = \frac{4}{\pi A}\int_{o}^{\pi/2} f_2(A \sin \sigma) \sin\sigma \, d\sigma$$

$$= \frac{4}{\pi A}\left[\int_{o}^{\theta_1} K_1 A \sin^2\sigma \, d\sigma + \int_{\theta_1}^{\frac{\pi}{2}} (K_1-K_2)X_1 \sin \sigma \, d\sigma + \int_{\theta_1}^{\frac{\pi}{2}} K_2 A \sin^2\sigma \, d\sigma \right]$$

Evaluating these integrals and rearranging gives

$$H(A) = \frac{2}{\pi} (\theta_1 - \frac{1}{2} \sin 2 \theta_1) (K_1-K_2) + K_2 + \frac{4}{\pi} (K_1-K_2) (\frac{X_1}{A}) \cos \theta_1 \qquad \ldots (I.20)$$

now,

$$x = A \sin \sigma$$

and when $\sigma = \theta_1$, $x = X_1$

$$\therefore \quad X_1 = A \text{ Sin } \theta_1$$

Hence,

$$\sin \theta_1 = \frac{X_1}{A}$$

and

$$\cos \theta_1 = \left[1 - (\frac{X_1}{A})^2 \right]^{\frac{1}{2}} \qquad (I.21)$$

Substituting $\sin \theta_1$ for $(\frac{X_1}{A})$ in (I.20) gives

$$H(A) = \frac{2}{\pi}(\theta_1 - \sin\theta_1\cos\theta_1)(K_1-K_2) + K_2 + \frac{4}{\pi}(K_1 - K_2)\sin\theta_1\cos\theta_1$$

$$= K_2 + \frac{2}{\pi}(K_1-K_2)\left[\theta_1 + \sin\theta_1\cos\theta_1\right]$$

Substituting values for θ_1, $\sin\theta_1$ and $\cos\theta_1$ in this expression, H(A) can be written as

$$H(A) = K_2 + \frac{2}{\pi}(K_1-K_2)\left[\sin^{-1}\left(\frac{X_1}{A}\right) + \left(\frac{X_1}{A}\right)\sqrt{1 - \left(\frac{X_1}{A}\right)^2}\right] \quad (I.22)$$

It is assumed that damping force does not change during a cycle. Hence,

$$f_1(\dot{x}) = c\,\dot{x}$$

$$G(A,\omega) = \frac{4}{\pi A}\int_0^{\frac{\pi}{2}} c(\omega A\cos\sigma)\cos\sigma\, d\sigma$$

on evaluating the above integral the following is obtained

$$G(A,\omega) = c\omega \quad (I.23)$$

Now substituting for H(A) and G(A,ω) from (I.22) and (I.23) respectively into (I.17) yields

$$\left[\frac{K_2}{M} + \frac{2}{\pi}\,\frac{K_1-K_2}{M}\left(\left(\frac{X_1}{A}\right)\sqrt{1 - \left(\frac{X_1}{A}\right)^2} + \sin^{-1}\left(\frac{X_1}{A}\right)\right) - \omega^2\right]^2 + \left(\frac{c\omega}{M}\right)^2 = \left[\frac{F}{MA}\right]^2 \quad (I.24)$$

Let $\frac{c}{M} = 2b$ and $d = \frac{b}{p_1}$ where $p_1^2 = \frac{K_1}{M}$

d is called damping factor or ratio of critical damping.

$$d = \frac{c}{2Mp_1}$$

or,

$$\frac{c}{M} = 2dp_1 \quad (I.25)$$

Substituting this value for $\frac{c}{M}$ in (I.24) gives

$$\left[\frac{K_2}{M} + \frac{2}{\pi}\left(\frac{K_1-K_2}{M}\right)\left(\left(\frac{X_1}{A}\right)\sqrt{1-\left(\frac{X_1}{A}\right)}\right) - \omega^2\right]^2 + (2dp_1\omega)^2 = \left[\frac{F}{MA}\right]^2$$

dividing this by p_1^4, ultimately gives

$$\left[\frac{K_2}{K_1} + \frac{2}{\pi}\left(\frac{K_1-K_2}{K_1}\right)\left(\left(\frac{X_1}{A}\right)\sqrt{1-\left(\frac{X_1}{A}\right)^2} + \sin^{-1}\left(\frac{X_1}{A}\right)\right) - \frac{\omega^2}{p_1^2}\right]^2 + \frac{4\,d^2\,\omega^2}{p_1^2} = \left[\frac{F}{K_1A}\right]^2 \qquad \text{(I.26)}$$

Also substituting proper values in (I.18) and rearranging, $\tan\psi$ can be written as

$$\tan\psi = \frac{\frac{2d\omega}{p_1}}{\frac{K_2}{K_1} + \frac{2}{\pi}\left(\frac{K_1-K_2}{K_1}\right)\left[\left(\frac{X_1}{A}\right)\sqrt{1-\left(\frac{X_1}{A}\right)^2} + \sin^{-1}\left(\frac{X_1}{A}\right)\right] - \frac{\omega^2}{p_1^2}} \qquad \text{. . .(I.27)}$$

APPENDIX - II

II-A Numerical Method for Determining Amplitude Response of the System After Any Number of Impacts

It is assumed that the duration of impact is very small so that the assumption at $t = o_+$ (+ sign represents the state, immediately after impact and - sign represents the state immediately preceding the impact), the positions of M and m remain the same while the respective absolute velocities are discontinuously changed from x_- and V_{m_-} (i.e. at $t = o_-$) to x_+ and V_{m_+} is justified. That the system does so has been verified experimentally as far as the positions of M and m are concerned, but there are enough evidences to believe (from the work of other investigators in this field, though for linear cases) that same is true for the case of velocities too (see references (3), (6)).

In Appendix - I, steady state motion of the system between impacts has been obtained by using Ritz averaging method[11]. Since the motion of the system during impact must satisfy the momentum equation, then

$$M\dot{x}_- + mV_{m_-} = M\dot{x}_+ + mV_{m_+} \tag{II.1}$$

and from the definition of coefficient of restitution e[12], the following relation is obtained,

$$\dot{x}_+ - V_{m_+} = -e(\dot{x}_- - V_{m_-}) \tag{II.2}$$

Dividing (II.1) by M and substituting μ for $\frac{m}{M}$ gives

$$\dot{x}_- + \mu V_{m_-} = \dot{x}_+ + \mu V_{m_+} \qquad \text{(II.3)}$$

(II.2) can be written as

$$e\,\dot{x}_- - e\,V_{m_-} = -\dot{x}_+ + V_{m_+} \qquad \text{(II.4)}$$

Adding (II.3) and (II.4) gives

$$(1+e)\dot{x}_- + (\mu-e)\,V_{m_-} = (1+\mu)\,V_{m_+}$$

or,

$$V_{m_+} = \left(\frac{1+e}{1+\mu}\right)\dot{x}_- + \left(\frac{\mu-e}{1+\mu}\right)V_{m_-} \qquad \text{(II.5)}$$

Substituting this value of V_{m_+} into (II.2) gives

$$\dot{x}_+ = \left(\frac{1+e}{1+\mu}\right)\dot{x}_- - e\,\dot{x}_- + \left(\frac{\mu-e}{1+\mu}\right)V_{m_-} + e\,V_{m_-}$$

or

$$\dot{x}_+ = \left(\frac{1-\mu e}{1+\mu}\right)\dot{x}_- + \frac{\mu(1+e)}{1+\mu}\,V_{m_-} \qquad \text{(II.6)}$$

Again substituting this value of $\dot{x}_+$ into (II.3) an expression for $\dot{x}_-$ in terms of variables V_{m_-} and V_{m_+} can be obtained. This is

$$\dot{x}_- = \frac{(e-\mu)V_{m_-} + (1+\mu)V_{m_+}}{(1+e)} \qquad \text{(II.7)}$$

Finally, an expression for $\dot{x}_+$ in terms of variables V_{m_-} and V_{m_+} can be obtained by substituting the value of $\dot{x}_-$ from (II.7) into (II.6). This gives

$$\dot{x}_+ = \frac{e(1+\mu)V_{m_-} + (1-\mu e)V_{m_+}}{(1+e)} \tag{II.8}$$

To summarize, impact condition must satisfy the following relations:

$$V_{m_+} = \left(\frac{1+e}{1+\mu}\right)\dot{x}_- + \left(\frac{\mu-e}{1+\mu}\right)V_{m_-} \tag{II.5}$$

$$\dot{x}_+ = \left(\frac{1-\mu e}{1+\mu}\right)\dot{x}_- + \frac{\mu(1+e)}{1+\mu}V_{m_-} \tag{II.6}$$

$$\dot{x}_- = \frac{(e-\mu)V_{m_-} + (1+\mu)V_{m_+}}{(1+e)} \tag{II.7}$$

$$\dot{x}_+ = \frac{e(1+\mu)V_{m_-} + (1-\mu e)V_{m_+}}{(1+e)} \tag{II.8}$$

Recalling the mathematical model in Figure 1, its equation of motion between impacts is

$$M\ddot{x} + f_1(\dot{x}) + f_2(x) = F \sin \omega t \tag{II.9}$$

$$\ddot{y} = -\ddot{x}\ * \tag{II.10}$$

where $f_1(\dot{x})$ and $f_2(x)$ stand for the damping force and spring force respectively.

If immediately after the i^{th} impact at $t = t_i$ the following variables assume the values

$$x(t_{i_+}) = x_i \ ; \quad y(t_{i_+}) = y_i \ ; \quad \dot{x}(t_{i_+}) = \dot{x}_i \ ; \quad \dot{y}(t_{i_+}) = \dot{y}_i \tag{II.11}$$

then the motion of M and m during the time interval from t_{i_+} to the time immediately preceding the next impact can be said to be given by

* See Appendix II-B for derivation.

$$x = A \sin(\omega t - \psi) \tag{II.12}$$

$$y = -x + (x_i + y_i) + (\dot{x}_i + \dot{y}_i)(t - t_i) \tag{II.13}$$

for $t_{i_+} < t < t_{(i+1)_-}$

It should however, be noted that x as given by (II.12) which was obtained by using Ritz averaging method in Appendix - I is not a complete solution of x, since it does not take into account the transients and gives only the steady state solution. However, for the present analysis, this approximation is justified.

The solution of (II.10) was obtained in the following way,

$$\ddot{y} = -\ddot{x}$$

$$\dot{y} = -\dot{x} + A_1$$

$$y = -x + A_1 t + A_2$$

applying initial conditions from (II.11)

$$\dot{y}_i = -\dot{x}_i + A_1 \qquad A_1 = \dot{y}_i + \dot{x}_i$$

$$\dot{y} = -\dot{x} + \dot{y}_i + \dot{x}_i \tag{II.14}$$

again applying initial conditions from (II.11)

$$y_i = -x_i + (\dot{y}_i + \dot{x}_i)t_i + A_2$$

$$A_2 = y_i + x_i - (\dot{y}_i + \dot{x}_i)t_i$$

Hence,

$$y = -x + (\dot{y}_i + \dot{x}_i)t + y_i + x_i - (\dot{y}_i + \dot{x}_i)t_i$$

$$y = -x + (x_i + y_i) + (\dot{x}_i + \dot{y}_i)(t - t_i) \; .$$

In order to obtain time behaviour of the system it is necessary to know the values of the variables in equations (II.12) and (II.13). The values of A and ψ are obtained from eqns. (I.26) and (I.27) in

Appendix - I. The other values can be obtained from impact condition.

Equation (II.6) gives the relationship between $\dot{x}_+$, $\dot{x}_-$ and V_{m_-}, that is

$$\dot{x}_+ = \left(\frac{1-\mu e}{1+\mu}\right)\dot{x}_- + \frac{\mu+\mu e}{1+\mu} V_{m_-} \tag{II.15}$$

but $V_m = \dot{y}_1$ (see Figure 1)

and $y_1 = y + x$

$$\therefore \quad V_m = \dot{y} + \dot{x} \tag{II.16}$$

Substituting this value of V_m in (II.1) gives

$$\dot{x}_+ = \left(\frac{1-\mu e}{1+\mu}\right) \dot{x}_- + \frac{\mu+\mu e}{1+\mu} \dot{x}_- + \frac{\mu+\mu e}{1+\mu} \dot{y}_-$$

Simplifying gives

$$\dot{x}_+ = \dot{x}_- + \frac{\mu(1+e)}{1+\mu} \dot{y}_- \tag{II.17}$$

Also (II.2) gives

$$\dot{y}_+ = -e \dot{y}_- \tag{II.18}$$

The impact condition at $t_{(i+1)_+}$ gives

$$x(t_{(i+1)_+}) = x(t_{(i+1)_-})$$

$$y(t_{(i+1)_+}) = y(t_{(i+1)_-}) \; ; \quad |y| = \frac{d_o}{2}$$

$$\dot{x}(t_{(i+1)_+}) = \dot{x}(t_{(i+1)_-}) + \left[\frac{\mu(1+e)}{(1+\mu)}\right] \dot{y}(t_{(i+1)_-}) \tag{II.19}$$

$$\dot{y}(t_{(i+1)_+}) = -e \, \dot{y}(t_{(i+1)_-})$$

Conditions (II.19) can now be used as new initial conditions in equations (II.12) and (II.13) for the time interval $t_{(i+1)_+}$ to $t_{(i+2)_-}$. This process can be repeated over and over again so as to obtain the time behaviour of the system.

II-B Derivation of Equation of Motion of the Mass Particle

Equation of motion of the mass particle can be obtained by using Lagrange's equation[16], which states

$$\frac{d}{dt}\left(\frac{\partial T}{\partial \dot{q}_r}\right) - \frac{\partial T}{\partial q_r} + \frac{\partial V}{\partial q_r} = Q_r \quad (r = 1, 2, \ldots n) \qquad \text{(II.20)}$$

where T = kinetic energy of the system

V = Potential energy of the system

q_r = Generalized co-ordinates

Q_r = Generalized forces at q_r which do not have potential.

Now, kinetic energy of the particle is given by

$$T = \frac{1}{2} m \dot{y}_1^2 \qquad \text{(II.21)}$$

$$\therefore \quad \frac{\partial T}{\partial \dot{y}_1} = m\dot{y}_1 \;, \text{ also } \frac{\partial T}{\partial y_1} = o \text{ and } \frac{\partial V}{\partial y_1} = o$$

$$\frac{d}{dt}\left(\frac{\partial T}{\partial \dot{y}_1}\right) = m\ddot{y}_1 = m(\ddot{y} + \ddot{x}) \qquad \text{(II.22)}$$

since $\ddot{y}_1 = \ddot{y} + \ddot{x}$ (see fig. 1).

Since $Q = o$ for the present case then substituting proper values into eqn. (II.20) gives

$$m(\ddot{y} + \ddot{x}) = o$$

$$\ddot{y} = -\ddot{x} \qquad \text{(II.23)}$$

APPENDIX - III

Experimental Results with 1" Diameter Ball and Different Clearances

Table III.1   Clearance d_o = 0.190"

Excitation frequency ω cycles/sec.	Single amplitude of vibration x in.	ω cycles/sec.	x in.
frequency increasing			
4	.039	7.1	.114
4.4	.037	7.2	.116
4.8	.042	7.3	.12
5.0	.044	7.4	.125
5.2	.0465	7.5	.126
5.4	.049	7.6	.129
5.6	.053	7.7	.133
5.8	.056	7.8	.135
6.0	.06	7.9	.138
6.2	.065	8.0	.1405
6.4	.07	8.1	.146
6.6	.07	8.2	.148
6.7	.074	8.3	.154
6.75	.082	8.4	.156
6.8	.095	8.5	.158
6.9	.104	8.6	.161
7.0	.109	8.7	.164

Table III.1 (continued)

ω	x	ω	x
8.8	.169	.	.
8.9	.1735	.	.
9.0	.177	.	.
9.1	.185	9.2	.039
9.15	.187	9.1	.042
9.2	.039	9.0	.044
9.3	.036	8.9	.047
9.4	.034	8.8	.051
9.5	.032	8.7	.054
9.6	.031	8.65	.052
9.7	.028	8.6	.055
9.8	.027	8.5	.058
9.9	.026	8.4	.063
10.0	.025	8.3	.069
10.2	.0225	8.2	.076
10.4	.021	8.1	.08
10.6	.02	8.0	.098
10.8	.018	7.95	.137
11.0	.016	7.8	.135
frequency decreasing		hereafter gave the same amplitude as during ω increasing.	
11.0	.016		
gave same amplitude as during ω increasing			

Table III.2 Clearance d_o = .330"

ω c/s frequency increasing	x in.	ω c/s	x in.
4.4	.0378	7.6	.129
4.8	.0404	7.7	.133
5.0	.0424	7.8	.1358
5.2	.0444	7.9	.137
5.4	.047	8.0	.1422
5.6	.0501	8.1	.146
5.8	.0535	8.2	.1475
6.0	.0574	8.3	.1514
6.2	.0621	8.4	.1528
6.4	.0652	8.5	.1566
6.6	.0678	8.6	.159
6.7	.073	8.65	.158
6.75	.0804	8.7	.162
6.8	.0856	8.8	.0535
6.85	.0878	8.9	.0483
6.9	.1044	9.0	.0456
7.0	.1096	9.1	.04175
7.1	.1135	9.2	.0378
7.2	.1174	9.4	.0352
7.3	.12	9.6	.0313
7.4	.124	9.8	.0282
7.5	.1266	10.0	.0256

Table III.2 (continued)

ω c/s	x in.
frequency increasing	
10.4	.02155
10.8	.0183
11.0	.017
frequency decreasing	
.	.
.	.
.	.
8.8	.0535
8.7	.0574
8.6	.064
8.5	.0705
8.4	.0782
8.3	.09
8.25	.0731
8.2	.0756
8.1	.0796
8.0	.09
7.9	.137
7.6	.129

hereafter gave the same amplitude as during ω increasing.

Table III.3 Clearance d_o = .500"

ω c/s	x in.	ω c/s	x in.
frequency increasing			
4.8	.0366	7.9	.1358
5.0	.0392	8.0	.1382
5.2	.043	8.1	.141
5.4	.0456	8.2	.1435
5.6	.0496	8.25	.1448
5.8	.0535	8.3	.146
6.0	.0574	8.35	.0861
6.2	.0652	8.4	.0809
6.4	.073	8.5	.0718
6.6	.0784	8.6	.0679
6.8	.0744	8.7	.0613
6.9	.0835	8.8	.0561
6.95	.1044	8.9	.0496
7.0	.1044	9.0	.047
7.1	.112	9.2	.0418
7.2	.115	9.4	.0366
7.3	.1175	9.6	.0313
7.4	.12	9.8	.0287
7.5	.124	10.0	.0261
7.6	.128	10.4	.0215
7.7	.131	10.8	.0183
7.8	.131	11.0	.017

Table III.3 (continued)

ω	x
frequency decreasing	
.	.
.	.
.	.
8.4	.081
8.3	.077
8.2	.0993
8.15	.1424
8.0	.1384
7.0	.1044
.	.
.	.
.	.

Table III.4 Clearance = .542"

ω c/s frequency	x in. increasing	ω c/s	x in.
4.4	.0366	7.6	.1305
4.8	.0382	7.7	.133
5.0	.0405	7.8	.136
5.2	.0418	7.9	.136
5.4	.0444	8.0	.1398
5.6	.047	8.1	.142
5.8	.051	8.2	.146
6.0	.0575	8.3	.150
6.2	.0548	8.4	.150
6.4	.0587	8.4	.0757
6.6	.0674	8.5	.0692
6.7	.0752	8.6	.0626
6.75	.0805	8.7	.0561
6.8	.0888	8.8	.0522
6.85	.098	9.0	.0444
6.90	.1045	9.2	.0378
7.0	.1084	9.4	.0339
7.1	.115	9.6	.0313
7.2	.116	9.8	.0282
7.3	.118	10.0	.0256
7.4	.1228	10.4	.0204
7.5	.1267	10.8	.0185

Table III.4 (continued)

ω	x
11.0	.017
frequency decreasing	
.	.
.	.
.	.
8.4	.0756
8.3	.0835
8.2	.0991
8.15	.1448
8.10	.1435
8.0	.138
.	.
.	.
.	.

APPENDIX - IV

A. Summary of Experimental Results With Same Ball Size but Different Clearances

Table IV-A.1 Ball diameter $D = \frac{5''}{8}$ ($A_{max} = 0.1906''$)

No. of observation	Clearance d_o inch	Gap factor $\frac{d_o}{A_{max}}$	Maximum Amplitude x in.	Amp. ratio $(\frac{x}{A})_{max}$
1	.423	2.222	.1893	.993
2	.700	3.672	.1867	.980
3	.797	4.180	.1865	.978
4	.919	4.820	.1789	.938
5	1.019	5.350	.1698	.890
6	1.095	5.750	.1722	.904
7	1.196	6.275	.1750	.917
8	1.295	6.80	.1750	.917

Table IV-A.2 Ball diameter $D = \frac{3''}{4}$

No. of observation	d_o inch	$\frac{d_o}{A_{max}}$	x in.	$(\frac{x}{A})_{max}$
1	.298	1.564	.1895	.994
2	.382	2.030	.1880	.986
3	.513	2.692	.1776	.932
4	.590	3.095	.1736	.910

Table IV-A.2 (continued)

No. of observation	d_o inch	$\frac{d_o}{A_{max}}$	x in.	$(\frac{x}{A})_{max}$
5	.698	3.665	.1723	.904
6	.762	4.000	.1645	.863
7	.814	4.270	.1593	.835
8	.905	4.750	.1567	.822
9	.960	5.040	.1567	.822
10	1.002	5.260	.1567	.822
11	1.087	5.700	.1643	.863

Table IV-A.3 Ball diameter $D = \frac{7''}{8}$

No. of observation	d_o	$\frac{d_o}{A_{max}}$	x	$(\frac{x}{A})_{max}$
1	.173	.9075	.1905	.999
2	.268	1.406	.1854	.972
3	.347	1.820	.1748	.916
4	.412	2.160	.1680	.880
5	.503	2.640	.1620	.850
6	.540	2.832	.1619	.850
7	.590	3.100	.1580	.828
8	.635	3.330	.1566	.822
9	.675	3.542	.1579	.827

Table IV-A.4 Ball diameter D = 1"

No. of observation	d_o	$\frac{d_o}{A_{max}}$	x	$(\frac{x}{A})_{max}$
1	.190	.997	.1870	.980
2	.265	1.390	.1800	.944
3	.310	1.627	.1696	.890
4	.330	1.731	.1620	.850
5	.395	2.071	.1540	.808
6	.463	2.430	.146	.766
7	.500	2.622	.146	.766
8	.542	2.84	.150	.787
9	.582	3.05	.153	.803

Table IV-A.5 Ball diameter D = $1\frac{1}{4}$"

No. of observation	d_o	$\frac{d_o}{A_{max}}$	x	$(\frac{x}{A})_{max}$
1	.066	.346	.1880	.986
2	.150	.787	.1775	.931
3	.205	1.076	.1657	.870
4	.264	1.384	.1553	.814
5	.290	1.521	.1461	.766
6	.313	1.642	.1383	.725
7	.347	1.820	.1358	.712
8	.381	2.000	.1423	.746

Table IV-A.6 Ball diameter $D = 1\frac{1}{2}''$

No. of observation	d_o	$\frac{d_o}{A_{max}}$	x	$(\frac{x}{A})_{max}$
1	.069	.362	.1761	.924
2	.145	.761	.1568	.822
3	.196	1.028	.1384	.726
4	.250	1.311	.1253	.675
5	.290	1.522	.1149	.6025
6	.312	1.640	.1096	.575

B. Summary of Experimental Results with Same Clearance but Different Balls

Table IV-B.1 Clearance $d_o = 0.351''$

No. of observation	Ball diameter D in.	Mass ratio* $\mu = \frac{m}{M}$	Amplitude ratio $(\frac{x}{A})_{max}$
1	5/8	.00822	1.0
2	3/4	.01436	.986
3	7/8	.0229	.973
4	1	.0337	.896
5	1 1/8	.0485	.725
6	1 1/4	.0668	.719
7	1 3/8	.0888	.688

* See Appendix IV.C

Table IV-B.2 Clearance $d_o = 0.403''$

No. of observation	Ball diameter D in.	Mass ratio $\mu = \frac{m}{M}$	Amplitude ratio $(\frac{x}{A})_{max}$
1	5/8	.00822	1.0
2	3/4	.01436	.972
3	7/8	.0229	.945
4	1	.0337	.876
5	1 1/4	.0667	.712

Table IV-B.3 Clearance $d_o = 0.500''$

No. of observation	D in.	μ	$(\frac{x}{A})_{max}$
1	1/2	.00417	.986
2	5/8	.00822	.979
3	3/4	.01546	.951
4	7/8	.0229	.876
5	1	.0337	.815
6	1 1/8	.0485	.725

C. Mass Ratios Between Different Balls and Primary System ($\mu = \frac{m}{M}$)

M = 4.3122 lb.

Ball diameter D in.	Mass of Ball m lb.	Mass ratio $\mu = \frac{m}{M}$
1/2	.018	.00417
5/8	.0355	.00822
3/4	.062	.01436
7/8	.099	.0229
1	.1455	.0337
1 1/8	.209	.0485
1 1/4	.288	.0667
1 3/8	.383	.0888
1 1/2	.496	.115

APPENDIX - V

A. Steady State Amplitude A and Phase-Angle ψ of the Primary System Without Impact Vibration Absorber (Analytical)

Table V.1 K_1 = 22 lb/in., K_2 = 60.2727 lb/in., X_1 = 0.104 in.
p_1 = 7.5 c/s, d = 0.045, F = 0.513 lb

A in.	ω_1 c/s	ω_2 c/s	ψ_1* rad	ψ_2* rad
.018	4.0830	11.3452	.06952	-.10528
.022	1.8393	10.7437	.02348	-.12193
.026	2.4141	10.3061	.03230	-.13833
.030	3.5488	9.9724	.05481	-.15457
.034	4.2163	9.7091	.07384	-.17070
.038	4.6773	9.4956	.09159	-.18677
.042	5.0204	9.3187	.10872	-.20280
.050	5.5028	9.0422	.14207	-.23481
.058	5.8292	8.8353	.17488	-.26687
.066	6.0665	8.6741	.20753	-.29905
.074	6.2477	8.5446	.24022	-.33142
.082	6.3911	8.4378	.27308	-.36405

* ψ_1 and ψ_2 corresponds to ω_1 and ω_2 respectively

Table V.1 (continued)

A	ω_1	ω_2	ψ_1	ψ_2
.090	6.5079	8.3480	.30618	-.39699
.098	6.6053	8.2712	.33961	-.43029
.106	6.7110	8.2227	.37480	-.46513
.114	6.9832	8.3247	.42210	-.51023
.122	7.2938	8.4770	.47567	-.56121
.130	7.5991	8.6411	.53331	-.61639
.138	7.8866	8.8028	.59449	-.65733
.146	8.1529	8.9563	.65930	-.73816
.154	8.3984	9.0989	.72828	-.80540
.162	8.6249	9.2297	.80243	-.87800
.170	8.8348	9.3482	.88342	-.95763
.178	9.0307	9.4540	.97417	-1.04717
.186	9.2164	9.5461	1.08049	-1.15241
.194	9.3983	9.6202	1.21766	-1.28862

B. <u>Time Behaviour of the Primary System with Impact Vibration Absorber</u>

Digital Computer Output

Table V.2 $\omega = 7.59917$ c/s, $p_1 = 7.5$ c/s, $d = 0.045$, $\mu = 0.0337$

$e = 0.8$, $A = 0.130$ in., $d_o = 0.50$ in., $A_{max} = 0.198$ in.

Impact (i)	t_i	x_i	y_i	x_{i_+}	y_{i_+}	$(\frac{x}{A})_{max}$ $t_{i-1} < t < t_i$
1	.0400	.12755	.25	2.1189	-12.5599	.6442
2	.1124	-.12900	-.25	.1100	8.9670	-.6515
3	.1915	.09259	.25	-3.5686	-10.7473	.4676
4	.2424	-.12986	-.25	-.5710	11.6814	-.6558
5	.3106	.12828	.25	-.2939	-9.6922	.6479
6	.3846	-.11057	-.25	2.4865	10.6002	-.5584
7	.4411	.12919	.25	.1196	-11.0204	.6525
8	.5103	-.12518	-.25	.9400	10.0632	-.6321
9	.5782	.12116	.25	-1.4712	-10.6017	.6119
10	.6402	-.12764	-.25	.3984	10.5991	-.6446
11	.7085	.12375	.25	-1.1440	-10.3189	.6250
12	.7738	-.12467	-.25	.9820	10.5766	-.6296
13	.8387	.12606	.25	-.7487	-10.4597	.6366
14	.9057	-.12415	-.25	1.0745	10.4389	-.6270
15	.9708	.12536	.25	-.8699	-10.5244	.6331
16	1.0367	-.12523	-.25	.8981	10.4470	-.6325
17	1.1028	.12471	.25	-.9832	-10.4776	.6298
18	1.1682	-.12531	-.25	.8815	10.4895	-.6329
19	1.2342	.12500	.25	-.9374	-10.4606	.6313

Table V.2 (continued)

Impact (i)	t_i	x_i	y_i	x_{i_+}	y_{i_+}	$(\frac{x}{A})_{max}$
20	1.3000	-.12499	-.25	.9368	10.4831	-.6312
21	1.3657	.12517	.25	-.9068	-10.4761	.6321
22	1.4316	-.12499	-.25	.9375	10.4708	-.6312
23	1.4973	.12507	.25	-.9229	-10.4800	.6317
24	1.5631	-.12509	-.25	.9208	10.4736	-.6317
25	1.6289	.12503	.25	-.9309	-10.4750	.6314
26	1.6947	-.12508	-.25	.9218	10.4771	-.6317
27	1.7605	.12506	.25	-.9255	-10.4742	.6316
28	1.8263	-.12505	-.25	.9268	10.4760	-.6316
29	1.8921	.12507	.25	-.9234	-10.4758	.6317
30	1.9579	-.12506	-.25	.9261	10.4750	-.6316
.	.	.	.	.	.	.
.	.	.	.	.	.	.
.	.	.	.	.	.	.
60	3.9318	-.12506	-.25	.9252	10.4755	-.6316
61	3.9976	.12506	.25	-.9252	-10.4755	.6316
62	4.0634	-.12506	-.25	.9252	10.4755	-.6316
.	.	.	.	.	.	.
.	.	.	.	.	.	.
.	.	.	.	.	.	.
100	6.4321	-.12506	-.25	.9252	10.4755	-.6316

APPENDIX - VI

A Method of Determining Coefficient of Restitution

Steady state speed of the mass particle can be said to be constant and is given by

$$v = (d_o + 2x_b)\,\frac{\omega}{\pi} \tag{VI.1}$$

If at $t = o_-$, the absolute velocity of the mass particle is represented by $V_{m_-} = v$ then at $t = o_+$, $V_{m_+} = -v$.

Now recalling

$$\dot{x}_- = \dot{x}_b,\quad \dot{x}_+ = \dot{x}_a$$

$$V_{m_-} = v,\quad V_{m_+} = -v$$

and substituting appropriate values in eqn. (II.7) gives

$$\dot{x}_b = \frac{v(e-1-2\mu)}{1+e} \tag{VI.2}$$

Using eqn. (VI.1) into (VI.2) ultimately gives

$$x_b + \frac{\pi}{2\omega}\left(\frac{1+e}{1-e+2\mu}\right)\dot{x}_b = -\frac{d_o}{2} \tag{VI.3}$$

Similarly from (II.8) $\dot{x}_a$ is given by

$$\dot{x}_a = \frac{v(e-1+2\mu e)}{1+e} \tag{VI.4}$$

and substituting for v from eqn. (VI.1) into eqn. (VI.4) ultimately gives

$$x_b + \frac{\pi}{2\omega}\left(\frac{1+e}{1-e-2\mu e}\right)\dot{x}_a = -\frac{d_o}{2} \tag{VI.5}$$

If eqn. (VI.5) be subtracted from (VI.3) it would give

$$(1-e-2\mu e)\ \dot{x}_b = (1-e+2\mu)\ \dot{x}_a$$

on simplification this gives

$$e = \frac{1-(1+2\mu)\dfrac{\dot{x}_a}{\dot{x}_b}}{(1+2\mu)-\dfrac{\dot{x}_a}{\dot{x}_b}} \qquad \text{(VI.6)}$$

from which e can be evaluated provided $\frac{\dot{x}_a}{\dot{x}_b}$ is known. The velocity ratio $(\frac{\dot{x}_a}{\dot{x}_b})$ in eqn. (VI.6) can be obtained by integrating with respect to time the output of an accelerometer attached to the primary mass M.

But since the value of e for hardened steel to hardened steel is known with quite a good accuracy and is equal to 0.8, this value of e (0.8) was taken for all theoretical calculations without actually determining it experimentally.

APPENDIX - VII

A. Experimental Technique

The RC signal generator in the test rig supplied the necessary voltage at a certain frequency to the input of the amplifier. The amplifier amplied this voltage, raised its energy level by means of push-pull operation and supplied current for energizing the exciter coil. This produced excitation to the model system corresponding to the voltage signal applied at the signal generator.

Amplitude of vibration of the primary system (i.e. relative motion between the mass and the foundation) was monitored by means of a capacitance transducer.

Any relative motion of the primary mass caused a proportional capacitance change of the transducer (considering the rest position of the system to correspond transducer's zero capacitance). The transducer's capacitance formed part of a series resonant circuit consisting of a fixed capacitance and an inductance. The combination of the fixed capacitance and an inductance together is referred here as tuning plug. This tuning plug was connected to an oscillator circuit through a co-axial cable. In the circuit diagram they can be represented as shown below

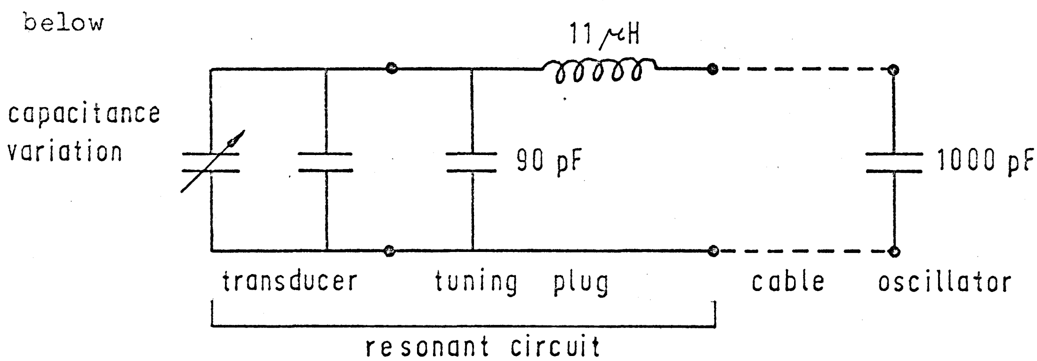

Fig. VII.1

Since f_c is given by $f_c = \frac{1}{2\pi\sqrt{LC}}$ where f_c is the resonant frequency of an electrical network, it is seen that the varying capacitance of the transducer in conjunction with a fixed reactance and a resonant circuit determined the frequency of the RF oscillator. In other words change in position of the primary mass was converted into a frequency change in the signal delivered by the oscillator. The frequency modulated signal was then fed to a reactance converter, which converted it into a DC voltage whose value followed the modulation of oscillator frequency. This DC voltage was then fed to the oscilloscope and was displayed onto the screen. The oscilloscope was previously calibrated in terms of its trace shift against known deflection of the mass and hence signal height on the screen gave a measure of the amplitude of vibration of the primary mass.

B. <u>List of Equipments used in Experimental Studies</u>

1. 1, Frequency Generator, "RC-Generator, type 29.060.69", Philips Gloeilampenfabrieken, Eindhoven, Holland.
2. 1, Amplifier Unit, "250 VA Amplifier type 119567", Philips.
3. 1, Ammeter.
4. 1, Vibration Generator (exciter), "Moving Coil Vibration Generator Model 790", Goodmans Industries Ltd. Wimbley, England.
5. 2, Capacitance Transducers (1, type 51D04-204 (co-axial) with a tuning plug type 51C02; 1, proximity Vibration Transducer type 51F21-136). DISA Elektronik, Herlev, Denmark.
6. 2, Oscillators, type 51E02-103, DISA Elektronik.
7. 2, Reactance Converters, type 51E01, DISA Elektronik.

8. 1, Cathode Ray Oscilloscope, Type 564 Storage Oscilloscope, Tektronix Inc. S. W. Millikan Way, Beaverton, Oregon, U. S. A.

APPENDIX - VIII

Digital Computer Result Together With Its

Experimental Equivalent

Table VIII.1 $\mu = 0.014360$ (3/4" dia. ball), $d_o = 0.513"$

ω rad/sec	x in. theoretical	experimental
5.0204	.034802	.0444
5.5028	.043698	.0502
5.8292	.052351	.0569
6.0665	.060801	.0613
6.2477	.069126	.0687
6.3911	.077433	.0757
6.5079	.085604	.0792
6.6053	.093804	.0830
6.9832	.110221	.1044
7.2938	.118181	.1187
7.5991	.128206	.1291
8.1529	.142388	.1448
8.6249	.158477	.1573
9.0307	.175074	.1761
9.2164	.185703 .166732	.0424
9.3983	.191648 .163587	.0378
9.3187	.034808	.03934

Table VIII.1 (continued)

ω rad/sec	x in. theoretical	experimental
9.0422	.043554	.0460
8.8353	.052351	.0575
8.5446	.069126	.0724
8.2227	.101972	.1002
8.4770	.118181	
8.6411	.128206	
8.8028	.134321	
8.9563	.142388	
9.2297	.158477	
9.3482	.166515	
9.4540	.175521	
9.5461	.185703 .166731	
9.6202	.191648 .163588	

Table VIII.2 $\mu = 0.0337$ (1" dia. ball), $d_o = 0.310"$

ω rad/sec	x in. theoretical	x in. experimental
5.0204	.037852	.044
5.5028	.046243	.0523
6.0665	.062686	.0653
6.5079	.087048	.0728
6.6053	.095105	.0745
6.9832	.111319	.1120
7.2938	.120040 .095908	.1200
7.5991	.125325 .093139	.1305
7.8866	.130278 .090540	.139
8.1529	.130893 .117676	.1446
8.6249	.153136 .139408	.1618
8.8348	.162628 .149803	.1679
9.0307	.171699 .159491	.044
9.2164	.180676 .169181	.039
9.3983	.189609 .179119	.034
10.3061	.020029	.0215
9.7091	.029184	.0294
9.0422	.046243	.0444
8.8353	.054502	.0522

ω rad/sec	x in. theoretical	experimental
8.2227	.103154	.0678
8.6411	.111376	
9.0989	.143097 .129124	
9.4540	.171699 .159492	
9.6202	.189608 .179120	

Table VIII.3 $\mu = 0.06670$ (1 1/4" dia. ball), $d_o = 0.210"$

ω rad/sec	x in. theoretical	x in. experimental
5.0240	.038440	.0522
5.5028	.046677	.0600
6.0665	.062949	.0707
6.5079	.087905 .060215	.0774
6.9832	.106057	.1122
7.2938	.115803	.1200
7.5991	.124255	.1305
7.8866	.134264	.1357
8.1529	.143788	.1500
8.6249	.161917	.1657
8.8348	.169459	.06
9.0307	.158474	.0509
10.7437	.016646	.02086
10.3061	.021296	.0222
9.7091	.030041	.0326
9.0422	.046677	.0494
8.5446	.071022	.0651
8.2227	.095278	.0752
8.3247	.106056	
8.6411	.124255	
8.9563	.143124	
9.3482	.169979	

APPENDIX - IX

Experimental Determination of the Structural Damping Factor

This was determined by measuring the peak amplitudes of free vibration of the system.

The free vibration trace of the system as displayed on the oscilloscope screen was photographed by a polaroid camera and peak amplitude for each cycle was measured. The value of damping factor was obtained by using the formula[15]

$$d = \frac{0.366}{k} \log_{10} \frac{r_1}{r_2}$$

where k = number of oscillations between two points 1 and 2 corresponding to maxima,

r_1 = maximum amplitude at point 1,

r_2 = maximum amplitude at point 2.

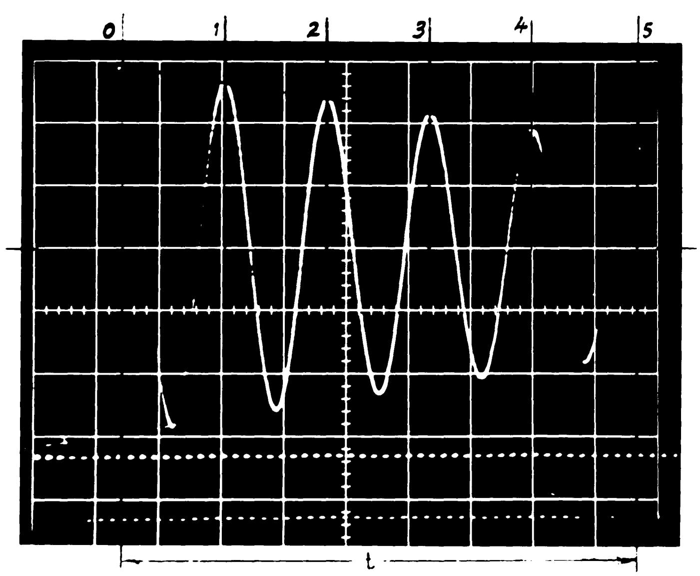

Fig. IX.1

From the above figure, the following data were obtained.

cycle no.	peak amplitude of vibration x k) (k = a constant)
0	1.05
1	.96
2	.86
3	.77
4	.68
5	.585

$$d_{o-1} = .366 \times \log_{10} \frac{1.05}{.96} = .366 \times .0386$$

$$= .0141$$

Similarly the others were calculated and d_{mean} was found to be,

$d_{mean} = 0.01854$

APPENDIX - X

COMPUTER PROGRAMMING

Programme - 1

Steady State Amplitude Response of the Mechanical System in Absence of Impact Vibration Absorber

This programme was written in order to solve for A and ψ at different frequencies ω from equation (I.26) and (I.27) respectively. For ease of solution ω was solved for known A.

Equation (I.26) was modified as

$$(Z_1 - c\,\omega^2)^2 + E\,\omega^2 - G = o, \tag{1}$$

where

$$Z_1 = \frac{K_2}{K_1} + \frac{2}{\pi}\,\frac{K_2-K_1}{K_1}\left[\frac{X_1}{A}\sqrt{1-\left(\frac{X_1}{A}\right)^2} + \sin^{-1}\left(\frac{X_1}{A}\right)\right]$$

$$c = \frac{1}{p_1^2}\,, \quad E = \frac{4\,d^2}{p_1^2}\,, \quad G = \left(\frac{F}{K_1 A}\right)^2$$

from eqn. (1)

$$\omega^2 = \frac{-Z_2 \pm \sqrt{(Z_2)^2 - Z_3}}{Z_4} = -\frac{Z_2}{Z_4} \pm \frac{\sqrt{D_2}}{Z_4} \tag{2}$$

where

$$Z_2 = E - 2cZ_1\,, \quad Z_3 = 4c^2(Z_1^2 - G)\,, \quad Z_4 = 2c^2$$

$$D_2 = (Z_2)^2 - Z_3$$

$$\omega^2 = BN \pm DN \tag{3}$$

where

$$BN = -\frac{Z_2}{Z_4}\,, \quad DN = \frac{\sqrt{D_2}}{Z_4}$$

Fortran Symbol	Actual Symbol Used in Mathematical Model
X1	X_1
FK1	F_1
FK2	F_2
F	F
P1	p_1
D	d
X	A
RWSQ1	ω_1^{2*} $(rad/sec)^2$
RWSQ2	ω_2^{2*} $(rad/sec)^2$
FREQ1	ω_1 (cycles/sec)
FREQ2	ω_2 (cycles/sec)
FR1	ω_1/p_1
FR2	ω_2/p_1
SHAI1	ψ_1**
SHAI2	ψ_2**

* ω_1 and ω_2 corresponds to two values of ω for one amplitude A.

** ψ_1 and ψ_2 corresponds to ω_1 and ω_2 respectively.

```
$JOB            003718 JHA              100    010    030
$IBJOB          NODECK
$IBFTC
C      STEADY STATE RESPONSE OF THE MECHANICAL SYSTEM HAVING
C      BI-LINEAR SPRING RESTORING FORCE
       X1=0.104
       FK1=22.0
       FK2=60.2727
       F=0.513
       G1=F*F
       G2=FK1*FK1
       G3=G1/G2
       P1=(2.0*3.1416*7.5)
       P=P1*P1
       C=1.0/P
       C1=C*C
       Z4=2.0*C1
       D=0.045
    70 E1=4.0*D*D
       E=E1/P
       X=0.016
       Z=0.5
       I=1
    10 X=X+Z*0.004
       X2=X*X
       G=G3/X2
```

```
      IF(X.GT.X1) GO TO 20
      A=1.0
      B=0.0
      B1=0.0
      GO TO 30
   20 A=FK2/FK1
      B=2.0*(FK1-FK2)/(3.1416*FK1)
      Q1=X1/X
      Q2=Q1*Q1
      R1=(1.0-Q2)
      R=R1**0.5
      U=ARSIN(Q1)
      B1=(Q1*R+U)
   30 Z1=A+B*B1
      Z5=Z1*Z1
      Z2=E-2.0*C*Z1
      Z3=4.0*C1*(Z5-G)
      D2=Z2*Z2-Z3
      BN=-Z2/Z4
      IF(D2.LT.0.0) GO TO 40
      DN=D2**0.5/Z4
      RWSQ1=BN+DN
      RWSQ2=BN-DN
      RW1=ABS(RWSQ1)**0.5
      RW2=ABS(RWSQ2)**0.5
      RPC=2.0*3.1416
```

```
      FREQ1=RW1/RPC
      FREQ2=RW2/RPC
      FR1=RW1/P1
      FR2=RW2/P1
      SHAI1=ATAN(2.0*D*FR1/(Z1-FR1*FR1))
      SHAI2=ATAN(2.0*D*FR2/(Z1-FR2*FR2))
      WRITE(6,2) X,FREQ2,FREQ1,SHAI2,SHAI1
    2 FORMAT(2X,F8.3,4E19.9)
      GO TO 50
   40 DN=(-D2)**0.5/Z4
      COMPR=BN
      COMP1=DN
      COMP2=-DN
      WRITE(6,3) X,COMPR,COMP1,COMP2
    3 FORMAT(2X,F8.3,3E19.9)
   50 IF(X.GE.0.04) Z=1.0
      I=I+1
      IF(I.EQ.80) GO TO 60
      GO TO 10
   60 WRITE(6,1)
    1 FORMAT(1H-)
      IF(D.EQ.0.050) GO TO 80
      D=0.050
      GO TO 70
   80 STOP
      END
$ENTRY
$IBSYS
```

Programme - 2

Steady State Amplitude Response of the System Provided with an Impact Vibration Absorber with Different Mass Ratios and Different Clearances

Fortran Symbol	Actual Symbol Used in Mathematical Model
BX	A (as obtained by executing programme - 1)
W1	ω_1
W2	ω_2
XMEW	μ
D	d_o
A	A_{max}
T	t
TI	t_+ (time immediately after impact)
XI	x_a
YI	y_a (relative position of the ball ω.r.t x immediately after impact)
XDOTI	$\dot{x}_a$
YDOTI	$\dot{y}_a$
E	e
X	x
Y	y
XDØT	$\dot{x}_b$
YDØT	$\dot{Y}_b$ (relative vel. of the ball immediately before impact)

Other symbols used are the same as in programme - 1.

```
$JOB            003718 JHA                  100   010   030
$IBJOB          NODECK
$IBFTC
C      AMPLITUDE RESPONSE OF THE MECHANICAL SYSTEM PROVIDED
C      WITH AN IMPACT VIBRATION ABSORBER.  THE VARIABLE PARAMETERS
C      ARE (1) 3/4 IN. DIA. BALL, 0.513 IN. CLEARANCE,
C      (2) 1 IN. DIA. BALL, 0.310 IN. CLEARANCE,
C      (3) 1 1/4 IN. DIA. BALL, 0.210 IN. CLEARANCE
      DIMENSION BX(104),W1(104),W2(104),SHAI1(104),SHAI2(104),XMEW(3)
     1D(3)
      READ(5,9) (XMEW(I),D(I),I=1,3)
    9 FORMAT(2F12.8)
      READ(5,1) (BX(I),W1(I),W2(I),SHAI1(I),SHAI2(I),I=1,52)
    1 FORMAT(5F12.8)
      DO 100 I=53,104
      BX(I)=BX(I-52)
      W1(I)=W2(I-52)
  100 SHAI1(I)=SHAI2(I-52)
      DO 20 N=1,3
      WRITE(6,4) XMEW(N),D(N)
    4 FORMAT(1H-,6H XMEW=,F20.9,3H D=,F20.9//)
      DO 20 I=9,104,2
      WRITE(6,7) BX(I),W1(I),SHAI1(I)
    7 FORMAT(2X,4H BX=,F20.9,7H OMEGA=,F20.9,7H SHAI1=,F20.9//)
      J=1
      M=1
```

```
      A=0.198
      T=0.0
      TI=0.0
      RPS=2.0*3.1416*W1(I)
      XI=0.0
      YI=D(N)/2.0
      XDOTI=0.0
      YDOTI=0.0
      E=0.8
      C=XMEW(N)*(1.0+E)/(1.0+XMEW(N))
   10 K=2
   11 T=TI+FLOAT(K-1)/100.0
      X=BX(I)*SIN(RPS*T-SHAI1(I))
      Y=-X+(XI+YI)+(XDOTI+YDOTI)*(T-TI)
      K=K+1
      IF((D(N)/2.0-ABS(Y)).LT.0.0) GO TO 45
      IF(K.GT.200) GO TO 45
      GO TO 11
   45 G=RPS*T
      IF(ABS(G).GT.2.0**25) GO TO 65
      X=BX(I)*SIN(RPS*T-SHAI1(I))
      F=(1.0/D(N))*(D(N)/2.0-ABS(-X+(XI+YI)+(XDOTI+YDOTI)*(T-TI)))
      XDOT=RPS*BX(I)*COS(RPS*T-SHAI1(I))
      DF=-(1.0/D(N))*ABS(-XDOT+(XDOTI+YDOTI))
      T=T-F/DF
      M=M+1
```

```
      IF(ABS(F).LE.1.E-6) GO TO 25
      IF(M.GT.80) GO TO 25
      GO TO 45
   65 WRITE(6,8) T,G
    8 FORMAT(2X,3H T=,E20.9,3H G=,E20.9)
      GO TO 35
   25 X= BX(I)*SIN(RPS*T-SHAI1(I))
      Y= -X+(XI+YI)+(XDOTI+YDOTI)*(T-TI)
      XDOT=RPS*BX(I)*COS(RPS*T-SHAI1(I))
      YDOT=-XDOT+YDOTI+XDOTI
      RATIO=X/A
      IF(J.LT.10) GO TO 55
      IF(ABS(ABS(XSS)-ABS(X)).LT.1.E-5) GO TO 35
      IF(ABS(ABS(X)-ABS(XSS)).LT.1.E-5) GO TO 35
   55 XSS=X
      M=1
      XI=X
      YI=Y
      XDOTI=XDOT+C*YDOT
      YDOTI=-E*YDOT
      TI=T
      WRITE(6,2) J,T,X, Y,XDOTI,YDOTI,RATIO
    2 FORMAT(2X,I3,6E19.8)
      J=J+1
      IF(J.GT.100) GO TO 35
      GO TO 10
```

```
   35 WRITE(6,3)
    3 FORMAT(1H-)
   20 CONTINUE
      STOP
      END
$ENTRY
0.14360      0.5130
0.03370      0.310
0.06670      0.210
```

0.018	4.0830648	11.345298	0.069523126	-0.10528772
0.020	3.0602138	11.018588	0.044029119	-0.11365221
0.022	1.8393682	10.743726	0.023480656	-0.12193854
0.024	1.2667682	10.509028	0.015646337	-0.13016297
0.026	2.4141950	10.306116	0.032307832	-0.13833787
0.028	3.0743170	10.128817	0.044313431	-0.14647295
0.030	3.5488139	9.9724766	0.054816152	-0.15457589
0.032	3.9174469	9.8335133	0.064556700	-0.16265292
0.034	4.2163072	9.7091256	0.073840123	-0.17070925
0.036	4.4654488	9.5970903	0.082822967	-0.17874908
0.038	4.6773549	9.4956162	0.091596293	-0.18677610
0.040	4.8603845	9.4032460	0.10021768	-0.19479344
0.042	5.0204279	9.3187805	0.10872578	-0.20280384
0.046	5.2877393	9.1697429	0.12550328	-0.21881279
0.050	5.5028488	9.0422912	0.14207120	-0.23481917
0.054	5.6802062	8.9319442	0.15851289	-0.25083617
0.058	5.8292641	8.8353863	0.17488163	-0.26687488

0.062	5.9565062	8.7501089	0.19121393	-0.28294503
0.066	6.0665477	8.6741785	0.20753633	-0.29905544
0.070	6.1627723	8.6060800	0.22386922	-0.31521426
0.074	6.2477217	8.5446093	0.24022883	-0.33142909
0.078	6.3233460	8.4887966	0.25662889	-0.34770736
0.082	6.3911676	8.4378523	0.27308121	-0.36405616
0.086	6.4523927	8.3911264	0.28959639	-0.38048261
0.090	6.5079917	8.3480787	0.30618443	-0.39699389
0.094	6.5587526	8.3082573	0.32285445	-0.41359716
0.098	6.6053238	8.2712801	0.33961546	-0.43029978
0.102	6.6482433	8.2368219	0.35647640	-0.44710929
0.106	6.7110935	8.2227256	0.37480182	-0.46513929
0.110	6.8366265	8.2627865	0.39738551	-0.48673349
0.114	6.9832520	8.3247695	0.42210766	-0.51023963
0.118	7.1377289	8.3979775	0.44830599	-0.53514813
0.122	7.2938608	8.4770356	0.47567077	-0.56121937
0.126	7.4483008	8.5587511	0.50403595	-0.58832408
0.130	7.5991742	8.6411037	0.53331334	-0.61639223
0.134	7.7454503	8.7227745	0.56346550	-0.64539609
0.138	7.8866068	8.8028946	0.59449118	-0.67533655
0.142	8.0224373	8.8808880	0.62641964	-0.70624334
0.146	8.1529335	8.9563805	0.65930416	-0.73816790
0.150	8.2782118	9.0291333	0.69322323	-0.77118593
0.154	8.3984725	9.0989967	0.72828590	-0.80540264
0.158	8.5139642	9.1658833	0.76462962	-0.84095178
0.162	8.6249720	9.2297406	0.80243411	-0.87800843

0.166	8.7318065	9.2905313	0.84193142	-0.91680454
0.170	8.8348006	9.3482237	0.88342267	-0.95763472
0.174	8.9343169	9.4027641	0.92731644	-1.0009062
0.178	9.0307583	9.4540630	0.97417504	-1.0471757
0.182	9.1245981	9.5019528	1.0248132	-1.0972593
0.186	9.2164447	9.5461259	1.0804972	-1.1524193
0.190	9.3071761	9.5859941	1.1433666	-1.2147919
0.194	9.3983488	9.6202780	1.2176688	-1.2886229
0.198	9.4938074	9.6453963	1.3146316	-1.3851390

$IBSYS

CD TOT 0159

Programme - 3

Steady State Amplitude Response of the System Provided with an Impact Vibration Absorber with a Single Mass Ratio and Different Clearances

Fortran symbols used in the programme are the same as in programme - 2.

N.B. Here the entry for BX(I), W1(I), W2(I), SHAI1(I), SHAI2(I) are the same as in programme - 2.

```
$JOB            003718 JHA                   100    010    030
$IBJOB          NODECK
$IBFTC
C     AMPLITUDE RESPONSE OF THE MECHANICAL SYSTEM PROVIDED
C     WITH AN IMPACT VIBRATION ABSORBER. VARIABLE PARAMETERS
C     ARE 1 IN. DIA. BALL AND CLEARANCES ARE (1) 0.2, (2) 0.4,
C     (3) 0.50 IN.
      DIMENSION BX(104),W1(104),W2(104),SHAI1(104),SHAI2(104),XMEW(3),
     1D(3)
      READ(5,9) (XMEW(I),D(I),I=1,3)
    9 FORMAT(2F12.8)
      READ(5,1) (BX(I),W1(I),W2(I),SHAI1(I),SHAI2(I),I=1,52)
    1 FORMAT(5F12.8)
      DO 100 I=53,104
      BX(I)=BX(I-52)
      W1(I)=W2(I-52)
  100 SHAI1(I)=SHAI2(I-52)
      DO 20 N=1,3
      WRITE(6,4) XMEW(N),D(N)
    4 FORMAT(1H-,6H XMEW=,F20.9,3H D=,F20.9//)
      DO 20 I=9,104,2
      WRITE(6,7) BX(I),W1(I),SHAI1(I)
    7 FORMAT(2X,4H BX=,F20.9,7H OMEGA=,F20.9,7H SHAI1=,F20.9//)
      J=1
      M=1
```

```
      A=0.198
      T=0.0
      TI=0.0
      RPS=2.0*3.1416*W1(I)
      XI=0.0
      YI=D(N)/2.0
      XDOTI=0.0
      YDOTI=0.0
      E=0.8
      C=XMEW(N)*(1.0+E)/(1.0+XMEW(N))
   10 K=2
   11 T=TI+FLOAT(K-1)/100.0
      X=BX(I)*SIN(RPS*T-SHAI1(I))
      Y=-X+(XI+YI)+(XDOTI+YDOTI)*(T-TI)
      K=K+1
      IF((D(N)/2.0-ABS(Y)).LT.0.0) GO TO 45
      IF(K.GT.200) GO TO 45
      GO TO 11
   45 G=RPS*T
      IF(ABS(G).GT.2.0**25) GO TO 65
      X=BX(I)*SIN(RPS*T-SHAI1(I))
      F=(1.0/D(N))*(D(N)/2.0-ABS(-X+(XI+YI)+(XDOTI+YDOTI)*(T-TI)))
      XDOT=RPS*BX(I)*COS(RPS*T-SHAI1(I))
      DF=-(1.0/D(N))*ABS(-XDOT+(XDOTI+YDOTI))
      T=T-F/DF
      M=M+1
```

```
      IF(ABS(F).LE.1.E-6) GO TO 25
      IF(M.GT.80) GO TO 25
      GO TO 45
   65 WRITE(6,8) T,G
    8 FORMAT(2X,3H T=,E20.9,3H G=,E20.9)
      GO TO 35
   25 X= BX(I)*SIN(RPS*T-SHAI1(I))
      Y= -X+(XI+YI)+(XDOTI+YDOTI)*(T-TI)
      XDOT=RPS*BX(I)*COS(RPS*T-SHAI1(I))
      YDOT=-XDOT+YDOTI+XDOTI
      RATIO=X/A
      IF(J.LT.10) GO TO 55
      IF(ABS(ABS(XSS)-ABS(X)).LT.1.E-5) GO TO 35
      IF(ABS(ABS(X)-ABS(XSS)).LT.1.E-5) GO TO 35
   55 XSS=X
      M=1
      XI=X
      YI=Y
      XDOTI=XDOT+C*YDOT
      YDOTI=-E*YDOT
      TI=T
      WRITE(6,2) J,T,X, Y,XDOTI,YDOTI,RATIO
    2 FORMAT(2X,I3,6E19.8)
      J=J+1
      IF(J.GT.100) GO TO 35
      GO TO 10
```

```
   35 WRITE(6,3)
    3 FORMAT(1H-)
   20 CONTINUE
      STOP
      END
$ENTRY
0.0337      0.20
0.0337      0.40
0.0337      0.50
$IBSYS
```

Programme - 4

Effect of Clearance (Gap Factor) on the Amplitude Response of the System at a Fixed Frequency

Fortran symbols used in the programme are the same as in the programme - 2.

```
$JOB            003718 JHA                  100    010    030
$IBJOB          NODECK
$IBFTC
C      EFFECT OF GAP FACTOR ON THE AMPLITUDE RESPONSE OF THE
C      SYSTEM AT A CERTAIN FREQUENCY, WHEN THE PARAMETER MASS
C      RATIO IS FIXED. THE INFORMATION OBTAINED FROM THIS
C      ANALYSIS CAN BE USED TO DETERMINE STABILITY BOUNDARIES
C      OF THE SYSTEM
       DIMENSION BX(30),W1(30),SHAI1(30),XMEW(30),D(30),E(30),A(30)
       READ(5,9) (BX(I),W1(I),SHAI1(I),XMEW(I),E(I),I=1,4)
     9 FORMAT(5F12.8)
       READ(5,12) (D(I),I=1,28)
    12 FORMAT(14F5.2)
       DO 20 I=1,4
       WRITE(6,7) BX(I),W1(I),SHAI1(I),XMEW(I),E(I)
     7 FORMAT(/2X,4H BX=,F13.9,7H OMEGA=,F14.9,7H SHAI1=,F13.9,
      16H XMEW=,F13.9,3H E=F13.9/)
       RPS=2.0*3.1416*W1(I)
       A(I)=BX(I)
       DO 20 N=22,28
       WRITE(6,4) D(N)
     4 FORMAT(2X,3H D=,F13.9/)
       M=1
       J=1
       T=0.0
       TI=0.0
```

```
      XI=0.0
      YI= D(N)/2.0
      XDOTI=0.0
      YDOTI=0.0
      C=XMEW(I)*(1.0+E(I))/(1.0+XMEW(I))
   10 K=2
   11 T=TI+FLOAT(K-1)/100.0
      X=BX(I)*SIN(RPS*T-SHAI1(I))
      Y=-X+(XI+YI)+(XDOTI+YDOTI)*(T-TI)
      K=K+1
      IF((D(N)/2.0-ABS(Y)).LT.0.0) GO TO 45
      IF(K.GT.200) GO TO 45
      GO TO 11
   45 G=RPS*T
      IF(ABS(G).GT.2.0**25) GO TO 65
      X=BX(I)*SIN(RPS*T-SHAI1(I))
      F=(1.0/D(N))*(D(N)/2.0-ABS(-X+(XI+YI)+(XDOTI+YDOTI)*(T-TI)))
      XDOT=RPS*BX(I)*COS(RPS*T-SHAI1(I))
      DF=-(1.0/D(N))*ABS(-XDOT+(XDOTI+YDOTI))
      T=T-F/DF
      M=M+1
      IF(ABS(F).LE.1.E-6) GO TO 25
      IF(M.GT.80) GO TO 25
      GO TO 45
   65 WRITE(6,8) T,G
    8 FORMAT(2X,3H T=,E20.9,3H G=,E20.9)
```

```
      GO TO 35
   25 X= BX(I)*SIN(RPS*T-SHAI1(I))
      Y= -X+(XI+YI)+(XDOTI+YDOTI)*(T-TI)
      XDOT=RPS*BX(I)*COS(RPS*T-SHAI1(I))
      YDOT=-XDOT+YDOTI+XDOTI
      RATIO=X/A(I)
      M=1
      XI=X
      YI=Y
      XDOTI=XDOT+C*YDOT
      YDOTI=-E(I)*YDOT
      TI=T
      WRITE(6,2) J,T,X, Y,XDOTI,YDOTI,RATIO
    2 FORMAT(2X,I3,6E19.8)
      J=J+1
      IF(J.GT.100) GO TO 35
      GO TO 10
   35 WRITE(6,3)
    3 FORMAT(1H-)
   20 CONTINUE
      STOP
      END
$ENTRY
0.130        7.599174020 0.53331334  0.03370      0.80
0.142        8.0224373   0.62641964  0.03370      0.80
0.158        8.5139642   0.76462962  0.03370      0.80
```

```
0.178        9.0307583   0.97417504  0.03370      0.80
0.1   0.2   0.3   0.4   0.5   0.6   0.7   0.8   0.9   1.0   1.1   1.2   1.3   1.4
1.5   1.6   1.7   1.8   1.9   2.0   2.1   2.2   2.3   2.4   2.5   2.6   2.7   2.8
$IBSYS
```

CD TOT   0094

REFERENCES

1. Lieber, P. and Jensen, D. P., "An Acceleration Damper: Development, Design, and Some Applications", Trans. ASME, Vol. 67 (1945), pp. 523-530.

2. Grubin, C., "On the Theory of the Acceleration Damper", Journal of Applied Mechanics, Vol. 23, Trans. ASME, Vol. 78 (1956), pp. 373-378.

3. Arnold, R. N., "Response of an Impact Vibration Absorber to Forced Vibration", Proceedings of 9th International Congress of Applied Mechanics, (1956), pp. 407-418.

4. Warbarton, G. B., Discussion of "On the Theory of the Acceleration Damper", Journal of Applied Mechanics, Vol. 24, Trans. ASME, Vol. 79 (1957), pp. 322-324.

5. Kaper, H. G., "The Behaviour of a Mass-Spring System Provided with a Discontinuous Dynamic Vibration Absorber", Applied Science Research, Section A, Vol. 10 (1961), pp. 369-383. (See also reference list of above paper.)

6. Masri, S. F., "Analytical and Experimental Studies of Impact Dampers", Ph.D. Thesis, California Institute of Technology (1965).

7. McGoldrick, R. T., "Experiments with an Impact Vibration Damper", David Taylor Model Basin Report No. 816.

8. Lieber, P. and Tripp, F., "Experimental Results on the Acceleration Damper", Rensselaer Polytechnic Institute Aeronautical Laboratory, Report No. 5401 (1954).

9. Sankey, G. O., "Some Experiments on a Particle or 'Shot' Damper", Memorandum, Westinghouse Research Labs. (1954).

10. Duckwald, C. S., "Impact Damping for Turbine Buckets", General Engineering Laboratory, General Electric, Report No. R55GL108 (1955).

11. Jacobsen, L. S., and Ayre, R. S., Engineering Vibrations with Applications to Structures and Machinery, McGraw-Hill Book Company, Inc. (1958), p. 283.

12. Housner, G. W. and Hudson, D. E., Applied Mechanics - Dynamics, D. Van Nostrand Company, Inc., Princeton, N. J., Third Edition (1955), p. 82.

13. Nielsen, K. L., Methods in Numerical Analysis, The Macmillan Company, Second Edition (1964), p. 175.

14. Nielsen, K. L., Methods in Numerical Analysis, The Macmillan Company, Second Edition (1964), p. 244.

15. Structural Damping; A Colloquium on Structural Damping held at the ASME annual meeting in December 1959, p. 120.

16. Bishop, R. E. D. and Johnson, D. C., The Mechanics of Vibration, (1960).